ASTRONOMY & ASTROPHYSICS
SUPPLEMENT SERIES

Astron. Astrophys. Suppl. Ser. **139**, 335–358 (1999)

The effective temperature scale of giant stars (F0–K5)

I. The effective temperature determination by means of the IRFM

A. Alonso, S. Arribas, and C. Martínez-Roger

Instituto de Astrofísica de Canarias, E-38200 La Laguna, Tenerife, Spain
e-mail: aas@ll.iac.es, sam@ll.iac.es and cmr@ll.iac.es

Received December 28, 1998; accepted July 5, 1999

Abstract. We have applied the InfraRed Flux Method (IRFM) to a sample of approximately 500 giant stars in order to derive their effective temperatures with an internal mean accuracy of about 1.5% and a maximum uncertainty in the zero point of the order of 0.9%. For the application of the IRFM, we have used a homogeneous grid of theoretical model atmosphere flux distributions developed by Kurucz (1993). The atmospheric parameters of the stars roughly cover the ranges: 3500 K $\leq T_{\rm eff} \leq$ 8000 K; $-3.0 \leq$ [Fe/H] $\leq +0.5$; $0.5 \leq \log(g) \leq 3.5$. The monochromatic infrared fluxes at the continuum are based on recent photometry with errors that satisfy the accuracy requirements of the work. We have derived the bolometric correction of giant stars by using a new calibration which takes the effect of metallicity into account. Direct spectroscopic determinations of metallicity have been adopted where available, although estimates based on photometric calibrations have been considered for some stars lacking spectroscopic ones. The adopted infrared absolute flux calibration, based on direct optical measurements of stellar angular diameters, puts the effective temperatures determined in this work in the same scale as those obtained by direct methods.

We have derived up to four temperatures, T_J, T_H, T_K and $T_{L'}$, for each star using the monochromatic fluxes at different infrared wavelengths in the photometric bands J, H, K and L'. They show good consistency over 4000 K, and there is no appreciable trend with wavelength, metallicity and/or temperature.

We provide a detailed description of the steps followed for the application of the IRFM, as well as the sources of error and their effect on final temperatures. We also provide a comparison of the results with previous work.

Key words: stars: fundamental parameters — stars: Population II — stars: atmospheres — stars: general

Send offprint requests to: A. Alonso

1. Introduction

The scale of temperatures of giant stars has been the target of a number of previous studies based on both **direct** and **indirect** methods (e.g. Ridgway et al. 1980; Bell & Gustafsson 1989; Blackwell et al. 1990; Mozurkewich et al. 1991; Richichi et al. 1992; Di Benedetto 1993, 1998; Dyck et al. 1998). In spite of these substantial efforts, very little attention has been paid to the role played by metallicity, especially in the case of *direct* methods given the restrictions on their application. Nevertheless, metallicity may have a non–negligible influence when applying the effective temperature scale to the analysis of important problems in astrophysics, such as the determination of chemical abundances from spectroscopy, the colour synthesis of stellar populations, the correct interpretation of the observed HR diagram and the observational test of stellar fluxes generated with atmospheric models.

The **direct** methods for measuring stellar angular diameters (i.e. mainly Michelson interferometry at different wavelengths and lunar occultation measurements) establish the empirical effective temperature scale of Population I giants ([Fe/H] $\sim$ 0) from G0III to M8III. Even in this case, on the observational side the error sources affecting the processes of measurement and reduction of the data make it difficult to ascertain such basic questions as whether spherical effects in the extended atmopsheres of the cooler stars are relevant. On the theoretical side the application of the limb–darkening correction remains unsure. This entails uncertainties concerning the nature of the stellar atmospheres in the range of late spectral types and low surface gravities. The present status for metal-poor giant stars is still more uncertain, given that no interferometric measurements of stellar diameters are available over the whole range of temperatures. A number of **indirect** methods based on stellar atmosphere models may be applied to determine

the effective temperatures of giant stars[1] (see for instance the review by Böhm-Vitense 1981). Unfortunately, theoretically based temperatures are not as trustworthy as would be desirable since atmosphere models cannot reproduce the observed fluxes with the required accuracy, especially in the UV range (e.g. Morossi et al. 1993). The suspicion that these problems are related to the adopted metal line opacities—a probable excess opacity for giants (Malagnini et al. 1992)—makes the temperature scale of metal-deficient stars more uncertain. In addition to their partial dependence on models, most of the previous works concerning the $T_{\rm eff}$ scale for metal–deficient giants have the additional drawback of the low number of stars. As a consequence, the uncertainties in the calibration of $T_{\rm eff}$ versus colour and metallicity are larger than desirable.

In order to overcome the above mentioned disadvantages, we have carried out a programme aimed at a more reliable definition of the effective temperature scale of giant stars (F0–K5). This work is part of a long term programme aimed at a complete revision of the $T_{\rm eff}$ scale of the different regions of the HR diagram. The work is based on the Infrared Flux Method (Blackwell et al. 1990), which has proven useful for deriving temperatures of metal-poor giants of globular clusters (Arribas & Martínez-Roger 1987; Arribas et al. 1991), and has low dependence on models for these types of stars. The temperatures obtained are scaled to *direct* $T_{\rm eff}$ (Alonso et al. 1994a; Paper II). A thorough account of the procedure followed for the application of the method can be found in (Alonso et al. 1996a; Paper I) where we described a similar programme devoted to main sequence stars.

As an initial step, we selected a sample of stars (~ 500) covering a wide range in metal content ($+0.5 > [{\rm Fe/H}] > -3.0$), and measured the infrared photometry $JHK(L')$ required for the application of the IRFM (Alonso et al. 1998; Paper IV). The number of stars and their distribution in the parameters space is adequate for establishing reliable relations $T_{\rm eff}$–colour–[Fe/H] for giant stars. In this paper, we present the temperatures obtained. In a forthcoming paper, we will provide and discuss the calibrations $T_{\rm eff}$–colour–[Fe/H], as well as the mean intrinsic colours for giant stars.

The present paper is laid out as follows. In Sects. 2, 3 and 4, we outline the practical implementation of the IRFM: i.e. the calibration of $q \times R$–factors by using the grid of atmosphere models computed by Kurucz (1991, 1993); The determination and calibration of bolometric fluxes of giant stars by applying a method previously devised to obtain and calibrate bolometric fluxes of main sequence stars (Alonso et al. 1995; Paper III) and the description of the assignment of secondary atmospheric parameters to the stars of the sample. The effective temperatures are derived in Sect. 5, where we provide an analysis of the the internal consistency of the method and the uncertainties affecting the derived efective temperatures. In Sect. 6, temperatures derived in the present work are compared with those derived in previous works. In Sect. 7, results are summarized.

[1] It is worth noting that, as implicitly mentioned, **direct** temperatures are not totally independent from models, since their determination demands limb–darkening corrections and the estimation of a part of the UV flux contributing to the bolometric flux.

2. The implementation of the IRFM

In principle, stellar effective temperatures can be determined in a fundamental way by measuring both the angular diameter and the bolometric flux of stars. In practice, this **direct** approach is limited to very bright stars confined to the close solar neighbourhood. If, as in the present programme, we are interested in extending the temperature determination to other target stars, then we are compelled to use **indirect** methods. Among the latter, the InfraRed Flux Method (Blackwell et al. 1990) has proven its reliability and non-critical dependence on models for spectral types earlier than late K and/or M. A detailed description of the implementation of the IRFM adopted in the present work is given in Paper I. For the sake of self-consistency we provide below a brief outline of it.

The determination of $T_{\rm eff}$ is obtained by comparing the quotient between the bolometric flux ($F_{\rm Bol}$) and the monochromatic flux at a chosen infrared wavelength of the continuum ($F(\lambda_{\rm IR})$) both measured at the top of the Earth's atmosphere ($R_{\rm obs}$), with the outputs of models ($R_{\rm theo}$). Therefore, the basic equation of the IRFM is:

$$R_{\rm obs} = \frac{F_{\rm Bol}}{F(\lambda_{\rm IR})} = \frac{\sigma T_{\rm eff}^4}{F_{\rm mod}(\lambda_{\rm IR}, T_{\rm eff}, [{\rm Fe/H}], g)} = \\ = R_{\rm theo}(\lambda_{\rm IR}, T_{\rm eff}, [{\rm Fe/H}], g), \quad (1)$$

where the dependence of models on metallicity, surface gravity, and $\lambda_{\rm IR}$ is explicitly taken into account. The monochromatic fluxes are obtained by applying the relation

$$F(\lambda_{\rm IR}) = q(\lambda_{\rm IR}, T_{\rm eff}, [{\rm Fe/H}], g)[F_{\rm cal}(\lambda_{\rm IR}) 10^{-0.4(m-m_{\rm cal})}], \quad (2)$$

where m and $m_{\rm cal}$ are, respectively, the magnitudes of the problem and standard star, $\lambda_{\rm IR}$ is the selected wavelength at the infrared, $F_{\rm cal}(\lambda_{\rm IR})$ is the absolute flux of the standard star at $\lambda_{\rm IR}$, and $q(\lambda_{\rm IR}, T_{\rm eff}, [{\rm Fe/H}], g)$ is a dimensionless factor which corrects the effect of the different curvature of the flux density distribution, across the filter window, between the standard and the problem stars.

The separation of observational and model inputs is easily obtained by substituting relation (2) in Eq. (1) as follows:

$$\frac{F_{\rm Bol}}{F_{\rm cal}(\lambda_{\rm IR}) 10^{-0.4(m-m_{\rm cal})}} = \\ = q(\lambda_{\rm IR}, T_{\rm eff}, [{\rm Fe/H}], g) R_{\rm theo}(\lambda_{\rm IR}, T_{\rm eff}, [{\rm Fe/H}], g). \quad (3)$$

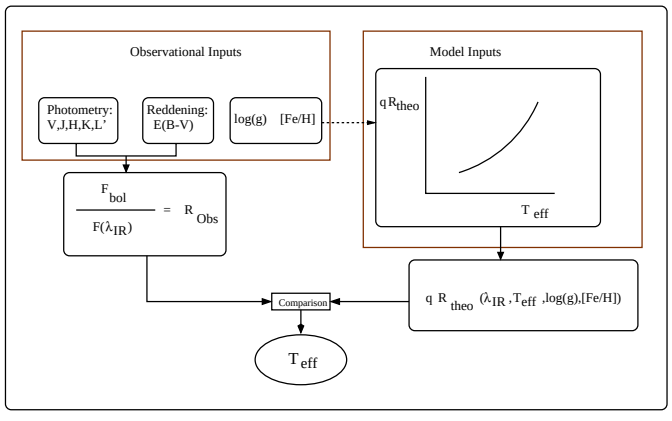

Fig. 1. Outline of the IRFM as implemented in the present work

Once [Fe/H] and $\log(g)$ are known for a certain star, the observational quantities on the left-hand side of Eq. (3) determine the star's effective temperature by comparing with the theoretical values obtained from models on the right-hand side. An outline of the practical application of the IRFM is shown in Fig. 1.

3. Model inputs: the q– and R–factors

The use of broad-band photometry to obtain the IR monochromatic fluxes requires the application of the so-called q-factors introduced in Eq. (2) (See also Paper I). Ideally, q-factors should be determined from spectroscopic data, but in the absence of a complete data base of empirical IR spectra, we have to rely on a grid of models to compute q -factors. Note however that q-factors always imply small corrections in the range studied.

The theoretical flux density distributions from Kurucz's (1991, 1993) models have been used to calculate $R_{\rm theo}(\lambda_{\rm IR})$ and $q(\lambda_{\rm IR})$ factors, as defined in Eq. (1) and Eq. (2) respectively. The effective wavelengths of the bands J, H, K and L' for the application of the IRFM were computed by considering the instrumental response of the photometric system (Alonso et al. 1994b and Paper IV) and the atmospheric transparency of the site computed by using the PLEXUS code (Clark 1996). Then the closest wavelengths sampled by the models were adopted ($\lambda_J = 1272.5$ nm, $\lambda_H = 1635.0$ nm, $\lambda_K = 2175.0$ nm and $\lambda_{L'} = 3690.0$ nm).

Tables 1, 2, 3 and 4 contain the calibration of q- and R-factors generated with Kurucz's models as a function of temperature, metallicity and surface gravity. Effective temperatures cover the range 3500−6500 K, surface gravities cover the range $\log(g) = (0.0 - 3.5)$, and metallicities cover the range (0.5, –3.5).

3.1. Sensitivity of $q \times R$ to the effective temperature

The separation of terms in Eq. (3) (i.e. model information to the right-handside, and observational data to the left-handside) is useful to simplify the analysis of the influence of errors on the derived temperatures.

Among the four near-IR wavelengths considered in this work, the $q \times R_J$ factors are the least sensitive to temperature, especially under 5000 K. The $q \times R_H$ and $q \times R_K$ sensitivities are comparable, although temperatures lower than 4000 K derived using $q \times R_H$ are less reliable, due to the relative maximum of the flux associated with the minimum of the H^- opacity reached in this band. As a consequence, the value of q_H factors in this temperature range is significantly different from 1, so that the effect of any possible uncertainty in the H^- opacity or in other sources of opacity which now become more important is amplified. Finally, the highest sensitivity to $T_{\rm eff}$ is shown by $q \times R_{L'}$, however this sensitivity is counterbalanced by the difficult of measurement of fluxes in this band.

The variations induced by the change in metallicity or surface gravity are only important for $T_{\rm eff}$ lower than 4250 K. In particular, the variation of R-factors in the range $\log(g) = 0 - 3.5$ for a fixed temperature and metallicity is almost negligible.

The values of $q \times R$ obtained from Tables 1–4 allow the errors induced by the uncertainties in the different input parameters of the IRFM on the derived temperatures to be derived easily (Fig. 2).
If we consider a variation of 5% in $q \times R$ —the theoretical counterpart to the quotient $F_{\rm Bol}/F(\lambda_{\rm IR})$— the change in temperatures derived using the factors R_H, R_K and $R_{L'}$ is practically constant over 4000 K: $1.6 - 2\%$ for T_H and 1.6% for T_K and $T_{L'}$. The change of T_J varies from 8% at 4000 K to 2% at 7000 K. Hence, R_J is the poorest indicator of $T_{\rm eff}$ for the application of the IRFM, and we will consider only T_J temperatures over 5000 K in the average. An uncertainty of 0.5 dex in metallicity causes, over 4000 K, a maximum average error of 0.5% in the mean temperatures derived applying the IRFM (Fig. 2). The influence of an error of 0.5 dex in $\log(g)$ is even smaller on the derived temperatures, reaching at most average errors of 0.3% over 4000 K.

4. Observational inputs for the IRFM

In the following paragraphs the different observational inputs which enter the application of the IRFM are commented on.

4.1. IR monochromatic fluxes

The determination of monochromatic fluxes at wavelengths of the IR continuum requires two observational inputs: Firstly, the measurement of IR photometry for the

Table 1. Calibration of $q-$ and $R-$factors versus metallicity, $\log(g)$ and effective temperature for $\lambda_{\rm eff}$ = 1272.5 nm (J band), computed using fluxes generated with Kurucz (1993) models

		[Fe/H]=0.50		[Fe/H]=0.00		[[Fe/H]=−1.00		[[Fe/H]=−2.00		[[Fe/H]=−3.00		[[Fe/H]=−3.50	
$T_{\rm eff}$	log(g)	q_J	log(R_J)	q_J	log(R_J)	q_J	log(R_J)	q_J	log(R_J)	q_J	log(R_J)	q_J	log(R_J)
3500	0.0	1.0129	3.20301	1.0093	3.24153	1.0050	3.27143	1.0061	3.25007	1.0076	3.21439	1.0074	3.17282
3750	0.0	1.0147	3.22904	1.0106	3.25793	1.0085	3.27145	1.0082	3.25031	1.0085	3.22490	1.0088	3.21854
4000	0.0	1.0155	3.24771	1.0130	3.26872	1.0105	3.27989	1.0085	3.26091	1.0080	3.24966	1.0082	3.24653
4250	0.0	1.0165	3.26798	1.0150	3.28540	1.0114	3.29781	1.0084	3.28732	1.0082	3.28382	1.0076	3.29357
4500	0.0	1.0173	3.29582	1.0159	3.31095	1.0113	3.32382	1.0084	3.32541	1.0078	3.32664	1.0077	3.32698
4750	0.0	1.0181	3.32971	1.0166	3.34234	1.0111	3.35573	1.0093	3.36046	1.0083	3.36304	1.0080	3.36364
5000	0.0	1.0184	3.36656	1.0170	3.37803	1.0108	3.39147	1.0091	3.39825	1.0083	3.40118	1.0081	3.40179
5250	0.0	1.0192	3.40483	1.0166	3.41549	1.0111	3.42963	1.0089	3.43728	1.0083	3.44029	1.0084	3.44084
5500	0.0	1.0194	3.44463	1.0168	3.45455	1.0116	3.46853	1.0090	3.47693	1.0085	3.47976	1.0086	3.48024
5750	0.0	1.0193	3.48627	1.0162	3.49671	1.0111	3.51172	1.0092	3.51924	1.0089	3.52226	1.0088	3.52295
6000	0.0	1.0182	3.53015	1.0151	3.54073	1.0106	3.55520	1.0090	3.56214	1.0086	3.56499	1.0085	3.56558
3500	1.0	1.0106	3.20247	1.0074	3.23941	1.0046	3.27609	1.0060	3.27523	1.0076	3.20371	1.0089	3.19402
3750	1.0	1.0126	3.23549	1.0093	3.26427	1.0074	3.28323	1.0070	3.28012	1.0076	3.24118	1.0086	3.21648
4000	1.0	1.0141	3.25985	1.0113	3.28051	1.0098	3.29301	1.0080	3.29221	1.0076	3.27231	1.0083	3.26835
4250	1.0	1.0151	3.28015	1.0132	3.29730	1.0106	3.31174	1.0079	3.31345	1.0082	3.30971	1.0080	3.30376
4500	1.0	1.0159	3.30441	1.0145	3.32039	1.0108	3.33718	1.0081	3.34103	1.0076	3.34228	1.0075	3.34290
4750	1.0	1.0166	3.33463	1.0152	3.34996	1.0107	3.36737	1.0082	3.37406	1.0074	3.37714	1.0073	3.37783
5000	1.0	1.0173	3.36973	1.0155	3.38342	1.0103	3.40091	1.0085	3.40919	1.0079	3.41275	1.0078	3.41352
5250	1.0	1.0177	3.40615	1.0155	3.41884	1.0105	3.43642	1.0088	3.44515	1.0084	3.44863	1.0082	3.44959
5500	1.0	1.0181	3.44317	1.0160	3.45541	1.0102	3.47311	1.0086	3.48158	1.0085	3.48510	1.0086	3.48572
5750	1.0	1.0190	3.48109	1.0158	3.49296	1.0103	3.50984	1.0088	3.51810	1.0083	3.52140	1.0084	3.52202
6000	1.0	1.0188	3.52033	1.0154	3.53278	1.0107	3.54924	1.0094	3.55737	1.0086	3.55834	1.0086	3.55862
6250	1.0	1.0175	3.56139	1.0148	3.57272	1.0104	3.58823	1.0092	3.59567	1.0088	3.59854	1.0088	3.59921
6500	1.0	1.0169	3.60296	1.0135	3.61389	1.0098	3.62814	1.0091	3.63446	1.0082	3.63726	1.0084	3.63777
6750	1.0	1.0154	3.64470	1.0122	3.65546	1.0091	3.66861	1.0083	3.67437	1.0076	3.67695	1.0077	3.67740
7000	1.0	1.0142	3.68541	1.0112	3.69563	1.0088	3.70771	1.0071	3.71344	1.0072	3.71566	1.0072	3.71612
3500	2.0	1.0088	3.19731	1.0063	3.23236	1.0057	3.27655	1.0089	3.27614	1.0105	3.21587	1.0104	3.19958
3750	2.0	1.0115	3.23417	1.0082	3.26268	1.0072	3.28628	1.0072	3.28795	1.0086	3.26688	1.0096	3.25882
4000	2.0	1.0128	3.26549	1.0103	3.28560	1.0089	3.29988	1.0080	3.30222	1.0082	3.29718	1.0086	3.29448
4250	2.0	1.0141	3.28945	1.0123	3.30506	1.0098	3.31964	1.0083	3.32400	1.0081	3.32227	1.0082	3.32170
4500	2.0	1.0151	3.31328	1.0136	3.32808	1.0101	3.34525	1.0080	3.35151	1.0082	3.35283	1.0077	3.35378
4750	2.0	1.0158	3.34128	1.0143	3.35595	1.0103	3.37466	1.0080	3.38317	1.0076	3.38696	1.0075	3.38781
5000	2.0	1.0161	3.37378	1.0144	3.38816	1.0101	3.40746	1.0081	3.41733	1.0075	3.42180	1.0075	3.42295
5250	2.0	1.0166	3.40862	1.0147	3.42239	1.0095	3.44235	1.0084	3.45239	1.0079	3.45693	1.0079	3.45788
5500	2.0	1.0173	3.44434	1.0150	3.45795	1.0096	3.47758	1.0084	3.48757	1.0084	3.49174	1.0083	3.49264
5750	2.0	1.0177	3.48087	1.0146	3.49418	1.0098	3.51306	1.0088	3.52238	1.0085	3.52626	1.0086	3.52711
6000	2.0	1.0172	3.51794	1.0145	3.53069	1.0099	3.54844	1.0088	3.55713	1.0087	3.56045	1.0088	3.56123
6250	2.0	1.0171	3.55606	1.0145	3.56726	1.0103	3.58379	1.0089	3.59174	1.0088	3.59475	1.0088	3.59547
6500	2.0	1.0171	3.59400	1.0139	3.60628	1.0106	3.62273	1.0094	3.63061	1.0091	3.62964	1.0093	3.63089
6750	2.0	1.0162	3.63315	1.0131	3.64442	1.0093	3.65996	1.0088	3.66660	1.0083	3.66958	1.0077	3.67043
7000	2.0	1.0149	3.67289	1.0118	3.68361	1.0087	3.69730	1.0081	3.70324	1.0080	3.70568	1.0072	3.70647
3500	3.0	1.0080	3.19320	1.0068	3.22765	1.0110	3.26299	1.0111	3.26657	1.0139	3.22221	1.2019	3.19163
3750	3.0	1.0109	3.22966	1.0083	3.25839	1.0082	3.28716	1.0098	3.28618	1.0100	3.28170	1.0101	3.27894
4000	3.0	1.0124	3.26542	1.0099	3.28630	1.0085	3.30198	1.0084	3.30562	1.0094	3.30342	1.0097	3.30222
4250	3.0	1.0138	3.29420	1.0117	3.30923	1.0096	3.32287	1.0087	3.32843	1.0085	3.32939	1.0088	3.32956
4500	3.0	1.0148	3.31962	1.0127	3.33335	1.0100	3.34877	1.0083	3.35642	1.0083	3.35891	1.0083	3.36002
4750	3.0	1.0155	3.34694	1.0135	3.36086	1.0100	3.37835	1.0082	3.38783	1.0079	3.39230	1.0079	3.39364
5000	3.0	1.0159	3.37759	1.0140	3.39160	1.0100	3.41089	1.0081	3.42175	1.0074	3.42719	1.0077	3.42851
5250	3.0	1.0160	3.41111	1.0141	3.42505	1.0096	3.44543	1.0079	3.45684	1.0077	3.46233	1.0077	3.46354
5500	3.0	1.0164	3.44616	1.0143	3.46003	1.0094	3.48076	1.0085	3.49216	1.0079	3.49727	1.0078	3.49849
5750	3.0	1.0169	3.48187	1.0139	3.49569	1.0095	3.51610	1.0086	3.52700	1.0083	3.53164	1.0083	3.53253
6000	3.0	1.0164	3.51814	1.0138	3.53136	1.0098	3.55121	1.0090	3.56119	1.0087	3.56522	1.0086	3.56625
6250	3.0	1.0159	3.55425	1.0132	3.56730	1.0099	3.58581	1.0092	3.59492	1.0089	3.59853	1.0089	3.59942
6500	3.0	1.0163	3.59003	1.0130	3.60304	1.0103	3.61994	1.0094	3.62807	1.0089	3.63155	1.0088	3.63241
6750	3.0	1.0151	3.62810	1.0130	3.63840	1.0098	3.65425	1.0090	3.66146	1.0083	3.66469	1.0089	3.66511
7000	3.0	1.0138	3.66536	1.0113	3.67745	1.0077	3.69401	1.0065	3.70168	1.0082	3.69821	1.0079	3.69970

problem stars with respect to a standard, and secondly the absolute flux calibration of the standard star. Then, entering the IR magnitudes measured in Eq. (2), we obtain monochromatic fluxes at λ_J, λ_H, λ_K and $\lambda_{L'}$ for each star in the sample.

In Paper II, a semi-empirical method was devised to determine the absolute calibration of the flux of Vega in the near-IR (from J to L'). This absolute calibration places temperatures derived applying the IRFM with Kurucz's models on the same scale as mean direct temperatures derived from angular diameter measurements. It is worth noting the good agreement (within 1%) with the semi-empirical calibration for Vega provided by Walker & Cohen (1992), the theoretical one by Dreiling & Bell (1980) and the "self-consistent" calibration by Blackwell et al. (1990).

The errors in the absolute IR flux calibration have different effects on the temperatures derived by mean of the IRFM, depending on the photometric band. The errors in the absolute IR flux calibration were estimated at 3% in the J band, 4% in H and K bands and 5% in L' band (Paper II). Over 4000 K, the net effect of

Table 2. The same as in Table 1 for $\lambda_{\rm eff} = 1635.0$ nm (H band)

		[Fe/H]=0.50		[Fe/H]=0.00		[[Fe/H]=−1.00		[[Fe/H]=−2.00		[[Fe/H]=−3.00		[[Fe/H]=−3.50	
$T_{\rm eff}$	log(g)	q_H	log(R_H)	q_H	log(R_H)	q_H	log(R_H)	q_H	log(R_H)	q_H	log(R_H)	q_H	log(R_H)
3500	0.0	1.0809	3.24181	1.1014	3.19886	1.1090	3.21063	1.0985	3.20598	1.0831	3.21060	1.0752	3.19415
3750	0.0	1.0693	3.31560	1.0831	3.27487	1.0880	3.28193	1.0790	3.27814	1.0682	3.28650	1.0642	3.29334
4000	0.0	1.0587	3.38351	1.0669	3.34713	1.0709	3.35102	1.0646	3.34561	1.0587	3.35524	1.0575	3.35641
4250	0.0	1.0499	3.44632	1.0538	3.41665	1.0579	3.41760	1.0539	3.41784	1.0521	3.42171	1.0502	3.43181
4500	0.0	1.0429	3.50529	1.0442	3.48407	1.0469	3.48653	1.0466	3.48968	1.0464	3.49191	1.0462	3.49228
4750	0.0	1.0366	3.56274	1.0376	3.54831	1.0398	3.55096	1.0412	3.55278	1.0415	3.55360	1.0415	3.55385
5000	0.0	1.0312	3.62016	1.0319	3.61431	1.0351	3.61343	1.0365	3.61555	1.0369	3.61632	1.0370	3.61650
5250	0.0	1.0301	3.67388	1.0280	3.67571	1.0312	3.67571	1.0326	3.67760	1.0326	3.67900	1.0324	3.67979
5500	0.0	1.0275	3.73124	1.0285	3.72847	1.0318	3.72755	1.0287	3.73948	1.0285	3.74126	1.0285	3.74161
5750	0.0	1.0257	3.78833	1.0269	3.78763	1.0300	3.78920	1.0305	3.79165	1.0303	3.79365	1.0303	3.79406
6000	0.0	1.0246	3.84500	1.0255	3.84644	1.0278	3.84964	1.0280	3.85264	1.0279	3.85424	1.0279	3.85457
3500	1.0	1.0923	3.21626	1.1051	3.19139	1.1109	3.20771	1.1006	3.22724	1.0799	3.21766	1.0665	3.24775
3750	1.0	1.0801	3.29199	1.0884	3.26787	1.0912	3.27986	1.0817	3.29795	1.0682	3.29984	1.0614	3.29757
4000	1.0	1.0683	3.36266	1.0726	3.34063	1.0727	3.35395	1.0669	3.36733	1.0581	3.37683	1.0553	3.38367
4250	1.0	1.0571	3.42862	1.0589	3.41016	1.0595	3.42160	1.0559	3.43532	1.0517	3.44726	1.0504	3.44497
4500	1.0	1.0479	3.49070	1.0487	3.47715	1.0495	3.48809	1.0480	3.49803	1.0468	3.50452	1.0468	3.50505
4750	1.0	1.0405	3.55016	1.0399	3.54444	1.0421	3.55145	1.0423	3.55899	1.0426	3.56126	1.0427	3.56173
5000	1.0	1.0337	3.61086	1.0344	3.60627	1.0364	3.61300	1.0386	3.61657	1.0386	3.61890	1.0384	3.61951
5250	1.0	1.0294	3.66787	1.0306	3.66551	1.0333	3.67072	1.0348	3.67412	1.0350	3.67588	1.0348	3.67713
5500	1.0	1.0265	3.72321	1.0278	3.72328	1.0306	3.72750	1.0317	3.73062	1.0314	3.73325	1.0315	3.73341
5750	1.0	1.0279	3.77210	1.0254	3.77906	1.0283	3.78308	1.0290	3.78701	1.0290	3.78859	1.0290	3.78900
6000	1.0	1.0269	3.82550	1.0277	3.82658	1.0305	3.83029	1.0306	3.83414	1.0273	3.84182	1.0267	3.84235
6250	1.0	1.0263	3.87815	1.0267	3.88038	1.0290	3.88483	1.0289	3.88865	1.0290	3.89011	1.0290	3.89051
6500	1.0	1.0259	3.93004	1.0262	3.93306	1.0277	3.93861	1.0277	3.94178	1.0277	3.94327	1.0277	3.94366
6750	1.0	1.0257	3.98007	1.0258	3.98416	1.0268	3.99040	1.0266	3.99378	1.0266	3.99532	1.0266	3.99566
7000	1.0	1.0256	4.02783	1.0254	4.03263	1.0260	4.03943	1.0257	4.04294	1.0257	4.04468	1.0257	4.04505
3500	2.0	1.0951	3.20160	1.1035	3.19081	1.1096	3.21743	1.0891	3.29148	1.0590	3.30117	1.0499	3.30451
3750	2.0	1.0824	3.27910	1.0878	3.26791	1.0890	3.28438	1.0795	3.31353	1.0596	3.35558	1.0486	3.38027
4000	2.0	1.0706	3.35203	1.0732	3.34139	1.0729	3.35532	1.0661	3.37644	1.0544	3.40975	1.0498	3.42369
4250	2.0	1.0592	3.42022	1.0600	3.41122	1.0597	3.42415	1.0553	3.44323	1.0477	3.46626	1.0463	3.47189
4500	2.0	1.0490	3.48473	1.0493	3.47788	1.0502	3.48964	1.0467	3.50778	1.0440	3.51995	1.0437	3.52173
4750	2.0	1.0409	3.54613	1.0412	3.54132	1.0424	3.55270	1.0413	3.56706	1.0408	3.57344	1.0407	3.57375
5000	2.0	1.0341	3.60555	1.0346	3.60358	1.0360	3.61468	1.0374	3.62338	1.0375	3.62706	1.0371	3.62869
5250	2.0	1.0292	3.66216	1.0297	3.66270	1.0330	3.67098	1.0339	3.67801	1.0336	3.68176	1.0336	3.68238
5500	2.0	1.0256	3.71761	1.0272	3.71865	1.0297	3.72612	1.0306	3.73154	1.0304	3.73483	1.0305	3.73533
5750	2.0	1.0233	3.77057	1.0246	3.77239	1.0273	3.77954	1.0278	3.78485	1.0280	3.78691	1.0280	3.78737
6000	2.0	1.0215	3.82197	1.0227	3.82503	1.0253	3.83131	1.0255	3.83629	1.0259	3.83781	1.0260	3.83836
6250	2.0	1.0232	3.86833	1.0212	3.87542	1.0232	3.88230	1.0236	3.88621	1.0237	3.88775	1.0237	3.88823
6500	2.0	1.0226	3.91816	1.0228	3.92146	1.0247	3.92804	1.0247	3.93187	1.0224	3.93632	1.0232	3.93593
6750	2.0	1.0222	3.96728	1.0221	3.97091	1.0238	3.97769	1.0238	3.98123	1.0238	3.98291	1.0238	3.98326
7000	2.0	1.0220	4.01515	1.0216	4.01970	1.0230	4.02611	1.0230	4.02958	1.0230	4.03112	1.0230	4.03140
3500	3.0	1.0965	3.19149	1.1015	3.19708	1.0774	3.31303	1.0577	3.35946	1.0520	3.32748	1.1033	3.30112
3750	3.0	1.0840	3.26743	1.0880	3.26612	1.0869	3.30664	1.0646	3.37300	1.0464	3.41121	1.0407	3.42247
4000	3.0	1.0724	3.34114	1.0744	3.33900	1.0726	3.35696	1.0614	3.39648	1.0432	3.45083	1.0372	3.46809
4250	3.0	1.0607	3.41199	1.0618	3.40882	1.0597	3.42487	1.0531	3.45110	1.0425	3.48820	1.0395	3.49944
4500	3.0	1.0501	3.47807	1.0509	3.47551	1.0496	3.49069	1.0446	3.51461	1.0396	3.53526	1.0387	3.53958
4750	3.0	1.0411	3.54081	1.0419	3.53951	1.0411	3.55486	1.0391	3.57399	1.0371	3.58554	1.0369	3.58786
5000	3.0	1.0340	3.60072	1.0348	3.60077	1.0356	3.61453	1.0352	3.62945	1.0346	3.63631	1.0343	3.63843
5250	3.0	1.0283	3.65822	1.0286	3.66028	1.0314	3.67174	1.0317	3.68357	1.0314	3.68829	1.0315	3.68903
5500	3.0	1.0236	3.71406	1.0250	3.71575	1.0277	3.72676	1.0283	3.73597	1.0287	3.73919	1.0287	3.73990
5750	3.0	1.0205	3.76675	1.0219	3.76921	1.0246	3.77933	1.0256	3.78653	1.0258	3.78933	1.0260	3.78975
6000	3.0	1.0182	3.81757	1.0191	3.82121	1.0217	3.83074	1.0225	3.83628	1.0229	3.83851	1.0229	3.83910
6250	3.0	1.0165	3.86685	1.0171	3.87118	1.0193	3.87986	1.0199	3.88472	1.0202	3.88663	1.0202	3.88723
6500	3.0	1.0149	3.91474	1.0154	3.92003	1.0173	3.92756	1.0178	3.93182	1.0180	3.93371	1.0179	3.93428
6750	3.0	1.0143	3.96113	1.0144	3.96615	1.0163	3.97360	1.0164	3.97767	1.0164	3.97947	1.0164	3.97989
7000	3.0	1.0134	4.00836	1.0133	4.01298	1.0155	4.02025	1.0157	4.02417	1.0152	4.02442	1.0151	4.02561

this systematic uncertainty is a drift of the temperature scale. If it happens that the above errors correlate in the three (four) bands, the maximum possible variation of the temperature scale would amounts to from 1.2% at 8000 K to 1.7% at 4000 K (1.3 − 1.7%) over 4000 K. However, if as it is more likely, the errors in the three (four) bands are uncorrelated, the net effect of the uncertainty of the absolute calibration would be an approximately constant shift in the zero point over the whole temperature range amounting to at most 0.9%. Although the indeterminacy of the zero point of the scale is common to all kind of methods used to derive effective temperatures, the method adopted in Paper II to fix the absolute calibration of the flux in the near IR was designed in order to minimising this error.

The programme of broad-band photometry in the near-IR is described in Paper IV. J, H, K (and L') magnitudes were measured for 70% of the stars in the sample, with a mean accuracy of the order of $0.01 - 0.02$ mag for J, H, K and 0.04 mag for L'. For the remainder of the stars, the photometry was obtained from the literature and transformed to the system of the TCS in order to compute near-IR monochromatic fluxes.

The isolated effect of the photometric errors on the $T_{\rm eff}$ determination can be inferred from Tables 1–4, taking Eq. (3) into account.

Table 3. The same as in Table 1 for $\lambda_{\rm eff} = 2175.0$ nm (K band)

		[Fe/H]=0.50		[Fe/H]=0.00		[[Fe/H]=−1.00		[[Fe/H]=−2.00		[[Fe/H]=−3.00		[[Fe/H]=−3.50	
$T_{\rm eff}$	log(g)	q_K	log(R_K)	q_K	log(R_K)	q_K	log(R_K)	q_K	log(R_K)	q_K	log(R_K)	q_K	log(R_K)
3500	0.0	1.0575	3.60479	1.0560	3.60904	1.0512	3.60753	1.0450	3.60304	1.0373	3.59442	0.3041	4.57645
3750	0.0	1.0552	3.68767	1.0536	3.68834	1.0480	3.68586	1.0409	3.68274	1.0321	3.68280	1.0273	3.68586
4000	0.0	1.0535	3.76477	1.0512	3.76322	1.0446	3.76114	1.0368	3.75676	1.0265	3.76171	1.0224	3.76154
4250	0.0	1.0512	3.83744	1.0481	3.83491	1.0408	3.83356	1.0314	3.83439	1.0209	3.83657	1.0193	3.84593
4500	0.0	1.0474	3.90676	1.0439	3.90454	1.0360	3.90725	1.0237	3.91087	1.0193	3.91177	1.0192	3.91202
4750	0.0	1.0428	3.97313	1.0390	3.97042	1.0292	3.97460	1.0202	3.97656	1.0194	3.97806	1.0195	3.97825
5000	0.0	1.0376	4.03674	1.0333	4.03772	1.0220	4.03935	1.0194	4.04177	1.0194	4.04323	1.0195	4.04342
5250	0.0	1.0318	4.09924	1.0266	4.09965	1.0200	4.10222	1.0194	4.10575	1.0195	4.10716	1.0198	4.10625
5500	0.0	1.0254	4.15927	1.0210	4.15846	1.0197	4.16066	1.0196	4.16788	1.0199	4.16823	1.0200	4.16842
5750	0.0	1.0208	4.21790	1.0192	4.21946	1.0194	4.22438	1.0192	4.22767	1.0194	4.22831	1.0193	4.22872
6000	0.0	1.0191	4.27630	1.0187	4.27977	1.0194	4.28556	1.0195	4.28816	1.0194	4.28975	1.0193	4.29016
3500	1.0	1.0548	3.59848	1.0532	3.60481	1.0487	3.61180	1.0427	3.62570	0.1704	4.92088	0.1794	4.88862
3750	1.0	1.0519	3.68155	1.0500	3.68492	1.0448	3.68978	1.0380	3.70374	0.9362	3.82638	0.3107	4.66793
4000	1.0	1.0494	3.75914	1.0470	3.76035	1.0407	3.76898	1.0339	3.77845	1.0260	3.77922	1.0224	3.78317
4250	1.0	1.0464	3.83196	1.0437	3.83202	1.0369	3.84080	1.0298	3.85140	1.0215	3.85874	1.0200	3.85423
4500	1.0	1.0432	3.90080	1.0402	3.90116	1.0334	3.91077	1.0245	3.91879	1.0195	3.92257	1.0193	3.92355
4750	1.0	1.0392	3.96660	1.0359	3.97035	1.0286	3.97682	1.0202	3.98285	1.0189	3.98547	1.0191	3.98578
5000	1.0	1.0347	4.03240	1.0316	4.03329	1.0230	4.03943	1.0192	4.04478	1.0192	4.04677	1.0190	4.04727
5250	1.0	1.0301	4.09271	1.0264	4.09372	1.0199	4.09995	1.0191	4.10465	1.0191	4.10637	1.0195	4.10552
5500	1.0	1.0251	4.15019	1.0214	4.15193	1.0193	4.15890	1.0190	4.16288	1.0194	4.16349	1.0192	4.16378
5750	1.0	1.0202	4.20584	1.0194	4.20844	1.0193	4.21546	1.0193	4.21855	1.0194	4.22009	1.0192	4.22057
6000	1.0	1.0178	4.26127	1.0173	4.26453	1.0183	4.27080	1.0184	4.27362	1.0189	4.27553	1.0188	4.27601
6250	1.0	1.0170	4.31618	1.0169	4.31996	1.0180	4.32653	1.0181	4.32939	1.0179	4.33215	1.0178	4.33256
6500	1.0	1.0168	4.36975	1.0168	4.37408	1.0182	4.38010	1.0179	4.38373	1.0178	4.38626	1.0178	4.38667
6750	1.0	1.0168	4.42170	1.0166	4.42670	1.0179	4.43316	1.0179	4.43673	1.0178	4.43905	1.0178	4.43941
7000	1.0	1.0168	4.47156	1.0165	4.47696	1.0179	4.48361	1.0178	4.48773	1.0176	4.48952	1.0178	4.48982
3500	2.0	1.0527	3.59843	1.0507	3.60616	1.0452	3.62468	1.0357	3.67618	0.2465	4.70604	0.3360	4.61703
3750	2.0	1.0489	3.68177	1.0472	3.68693	1.0422	3.69640	1.0341	3.71562	1.0265	3.73678	1.0243	3.75049
4000	2.0	1.0456	3.75999	1.0437	3.76315	1.0381	3.77149	1.0308	3.78516	1.0240	3.80528	1.0220	3.81395
4250	2.0	1.0424	3.83289	1.0400	3.83507	1.0342	3.84358	1.0277	3.85684	1.0220	3.86990	1.0206	3.87368
4500	2.0	1.0392	3.90165	1.0365	3.90355	1.0308	3.91276	1.0242	3.92459	1.0201	3.93272	1.0196	3.93441
4750	2.0	1.0355	3.96720	1.0329	3.96892	1.0274	3.97816	1.0207	3.98874	1.0191	3.99406	1.0192	3.99412
5000	2.0	1.0319	4.02981	1.0295	4.03205	1.0230	4.04093	1.0192	4.04978	1.0189	4.05287	1.0193	4.05216
5250	2.0	1.0279	4.08945	1.0253	4.09124	1.0199	4.10106	1.0187	4.10771	1.0191	4.10885	1.0192	4.10938
5500	2.0	1.0237	4.14582	1.0210	4.14900	1.0189	4.15798	1.0189	4.16353	1.0192	4.16451	1.0192	4.16499
5750	2.0	1.0199	4.20053	1.0187	4.20418	1.0188	4.21291	1.0188	4.21668	1.0188	4.21872	1.0188	4.21916
6000	2.0	1.0173	4.25351	1.0175	4.25778	1.0180	4.26605	1.0181	4.26956	1.0182	4.27257	1.0181	4.27313
6250	2.0	1.0145	4.30764	1.0168	4.30925	1.0180	4.31624	1.0181	4.32042	1.0178	4.32339	1.0179	4.32381
6500	2.0	1.0140	4.35899	1.0140	4.36357	1.0157	4.37019	1.0155	4.37441	1.0172	4.37375	1.0169	4.37494
6750	2.0	1.0135	4.40965	1.0134	4.41432	1.0150	4.42113	1.0151	4.42613	1.0150	4.42788	1.0150	4.42824
7000	2.0	1.0132	4.45899	1.0130	4.46335	1.0147	4.47064	1.0146	4.47537	1.0146	4.47692	1.0145	4.47727
3500	3.0	1.0525	3.59667	1.0467	3.61069	1.0377	3.68837	1.0314	3.71625	2.2592	3.67961	0.4044	4.42095
3750	3.0	1.0474	3.67877	1.0440	3.68595	1.0361	3.71601	1.0286	3.75739	1.0247	3.77780	1.0236	3.78391
4000	3.0	1.0441	3.75692	1.0412	3.76196	1.0345	3.77333	1.0271	3.79877	1.0228	3.83145	1.0223	3.84198
4250	3.0	1.0405	3.83078	1.0379	3.83406	1.0312	3.84451	1.0249	3.86094	1.0213	3.88380	1.0209	3.89100
4500	3.0	1.0364	3.89991	1.0339	3.90268	1.0282	3.91312	1.0229	3.92798	1.0205	3.94140	1.0203	3.94418
4750	3.0	1.0325	3.96545	1.0302	3.96824	1.0256	3.97819	1.0208	3.99234	1.0198	4.00032	1.0195	4.00203
5000	3.0	1.0290	4.02784	1.0271	4.03074	1.0226	4.04081	1.0195	4.05302	1.0192	4.05798	1.0196	4.05781
5250	3.0	1.0255	4.08749	1.0238	4.08985	1.0200	4.10104	1.0190	4.11061	1.0194	4.11275	1.0195	4.11338
5500	3.0	1.0218	4.14385	1.0203	4.14699	1.0187	4.15799	1.0189	4.16423	1.0191	4.16716	1.0190	4.16784
5750	3.0	1.0183	4.19812	1.0178	4.20204	1.0183	4.21231	1.0186	4.21735	1.0183	4.22004	1.0181	4.22208
6000	3.0	1.0154	4.25084	1.0160	4.25495	1.0176	4.26332	1.0177	4.26896	1.0175	4.27279	1.0176	4.27334
6250	3.0	1.0140	4.30115	1.0150	4.30588	1.0166	4.31381	1.0169	4.31881	1.0169	4.32230	1.0170	4.32280
6500	3.0	1.0133	4.34995	1.0142	4.35418	1.0155	4.36278	1.0157	4.36864	1.0158	4.37056	1.0158	4.37104
6750	3.0	1.0093	4.40321	1.0129	4.40220	1.0143	4.41041	1.0147	4.41568	1.0149	4.41736	1.0149	4.41777
7000	3.0	1.0084	4.45033	1.0084	4.45569	1.0101	4.46418	1.0105	4.46980	1.0134	4.46396	1.0131	4.46566

4.2. Bolometric fluxes

For the range of spectral types studied in the present work, nearly all the flux arriving at the earth atmosphere passes through the atmospheric windows. When comparing $F_{\rm Bol}$ derived directly from calibrated spectra to $F_{\rm Bol}$ obtained by integrating $UBVRI$ photometry, Petford et al. (1988) report an accuracy of the order of 2%. Therefore, the bolometric flux might be obtained for each star in the sample from broad-band photometry. However, photometric calibrations of the type provided by Blackwell & Petford (1991) and Blackwell & Lynas-Gray (1998) represent a more practical and accurate approach. We have obtained calibrations of this kind by fitting the bolometric fluxes of 184 stars of the sample, well distributed in metallicity, as a function of K, $(V-K)$ and [Fe/H]. Bolometric fluxes ($F_{\rm Bol}$) have been obtained by integrating $UBVRIJHK$ photometry. The percentage of $F_{\rm Bol}$ measured in U—K bands ranges from 80% to 90% for the giant stars contained in our sample. The energy outside that wavelength range (i.e. UV and far IR flux) has been estimated with the help of models as described thoroughly in Paper III. The low dispersion of the fits grants the overall level of accuracy expected for the final temperatures derived in

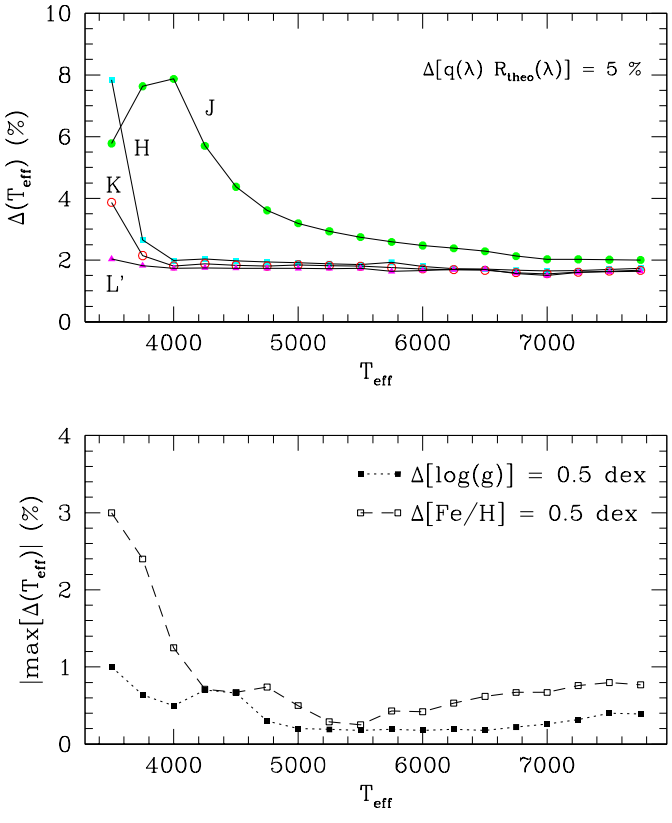

Fig. 2. Top: Mean uncertainties in the IRFM temperatures derived from J, H, K and L' fluxes, induced by an error of 5% in the observational quotient $\frac{F_{\rm Bol}}{F_{\rm cal}(\lambda_{\rm IR})10^{-0.4(m-m_{\rm cal})}}$. Bottom: Maximum mean uncertainties of the IRFM temperatures induced by an error of 0.5 dex in [Fe/H] and $\log(g)$ respectively. Note the change in the scale of the ordinate axis with respect to the top figure

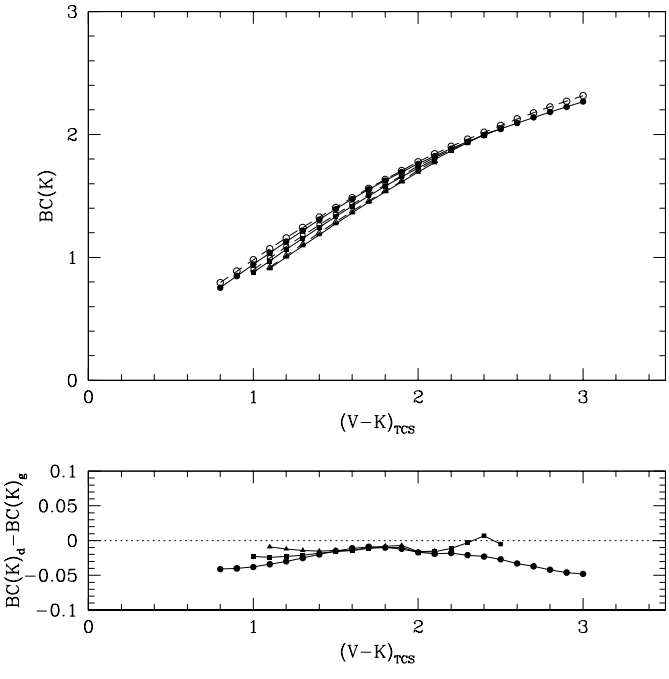

Fig. 3. Top: Bolometric correction to $K_{\rm TCS}$ versus $(V-K)_{\rm TCS}$. Solid circles correspond to dwarf stars and open circles to giant stars. Circles: [Fe/H] = 0.0; squares: [Fe/H] = −1.5; triangles: [Fe/H] = −3.0. Bottom: Difference between the bolometric correction to $K_{\rm TCS}$ of dwarf and giant stars

this work[2]. The result of the calibration for $(V-K) \leq 2.1$ is

$$\begin{aligned}\log(\Phi(K)) = &-4.5939829 - 0.4560143(V-K)\\ &-3.251330\ 10^{-2}[\mathrm{Fe/H}]\\ &+1.1160121\ 10^{-2}[\mathrm{Fe/H}](V-K)\\ &+4.6114362\ 10^{-2}(V-K)^2 \qquad (4)\\ &\sigma = 0.006 \approx 1.5\%, 50\ \text{stars}.\end{aligned}$$

If we consider only stars with $(V-K) \geq 2.0$, then

$$\begin{aligned}\log(\Phi(K)) = &-4.6538559 - 0.4152091(V-K)\\ &-1.6208590\ 10^{-2}[\mathrm{Fe/H}]\\ &+4.1133101\ 10^{-3}[\mathrm{Fe/H}](V-K)\end{aligned}$$

$$\begin{aligned}&+4.0213845\ 10^{-2}(V-K)^2 \qquad (5)\\ &\sigma = 0.006 \approx 1.5\%, 141\ \text{stars},\end{aligned}$$

where $\Phi(K)$ is the so-called reduced flux to magnitude K, defined through the equation $F_{\rm Bol} = 10^{-0.4\,K}\Phi(K)$. It should be noted that these calibrations are ultimately based on the optical absolute flux calibrations of Vega by Hayes & Latham (1975) and Tüg et al. (1977), and the IR absolute flux measured in Paper II.

The corresponding bolometric correction for $K_{\rm TCS}$ magnitudes for giant stars obtained from Eqs. (4) and (5) is listed in Table 5, where the validity range of the calibration, in colour and metallicity, is shown. The differences from the bolometric correction obtained by applying the same method to main sequence stars are in the range $0.01 - 0.05$ mag (Fig. 3).

In Fig. 4 we show the difference between bolometric corrections or fluxes derived here, and those from the following authors:

Bessell, Castelli and Plez (1998; BCP98)

This work comprehensively provides bolometric corrections synthesized from different grids of stellar model fluxes of solar metallicity. The comparison of the BC(K) scales in Fig. 4a shows a consistent agreement in the range

[2] Hereafter in this section, K and $(V-K)$ are in the TCS system. Transformations from TCS to other systems are well described in Paper IV, in particular for the Johnson system: $K_{\rm TCS} = K_J - 0.042 + 0.019(J-K)_J$, and $(V-K)_{\rm TCS} = 0.050 + 0.993(V-K)_J$.

Table 4. The same as in Table 1 for $\lambda_{\rm eff} = 3690.0$ nm (L' band)

		[Fe/H]=0.50		[Fe/H]=0.00		[[Fe/H]=−1.00		[[Fe/H]=−2.00		[[Fe/H]=−3.00		[[Fe/H]=−3.50	
$T_{\rm eff}$	log(g)	$q_{L'}$	log($R_{L'}$)	$q_{L'}$	log($R_{L'}$)	$q_{L'}$	log($R_{L'}$)	$q_{L'}$	log($R_{L'}$)	$q_{L'}$	log($R_{L'}$)	$q_{L'}$	log($R_{L'}$)
3500	0.0	0.9980	4.43201	1.0002	4.44019	1.0052	4.43689	0.9440	5.31112	1.0288	5.37874	1.0298	5.39615
3750	0.0	0.9964	4.52257	0.9991	4.52605	1.0050	4.51965	0.9489	5.36607	1.0253	5.32900	1.0253	5.31477
4000	0.0	0.9946	4.60545	0.9978	4.60534	1.0043	4.59802	0.9553	5.40304	1.0222	5.29304	1.0209	5.19871
4250	0.0	0.9942	4.68165	0.9977	4.67927	1.0041	4.67238	0.9634	5.40786	1.0173	5.21546	1.0084	4.67022
4500	0.0	0.9941	4.75293	0.9977	4.74959	1.0048	4.74428	1.0069	4.74289	1.0070	4.74369	1.0075	4.74357
4750	0.0	0.9946	4.81979	0.9985	4.81548	1.0047	4.81257	1.0061	4.81335	1.0065	4.81357	1.0070	4.81353
5000	0.0	0.9953	4.88300	0.9989	4.88035	1.0046	4.87812	1.0059	4.88024	1.0062	4.88086	1.0062	4.88108
5250	0.0	0.9951	4.94791	0.9992	4.94149	1.0041	4.94215	1.0053	4.94438	1.0056	4.94559	1.0052	4.94598
5500	0.0	0.9957	5.00739	0.9986	5.00660	1.0024	5.00829	1.0045	5.00590	1.0045	5.00727	1.0045	5.00739
5750	0.0	0.9961	5.06580	0.9988	5.06629	1.0022	5.06964	1.0033	5.07258	1.0035	5.07412	1.0033	5.07461
6000	0.0	0.9963	5.12282	0.9984	5.12511	1.0016	5.12965	1.0025	5.13276	1.0027	5.13432	1.0025	5.13481
3500	1.0	0.9987	4.42786	1.0020	4.43654	1.0063	4.43919	0.9940	4.54230	1.0268	5.24524	1.0265	5.22568
3750	1.0	0.9975	4.51901	0.9999	4.52441	1.0053	4.52358	1.0078	4.52446	1.0234	5.20838	1.0220	5.13232
4000	1.0	0.9957	4.60294	0.9989	4.60478	1.0050	4.60371	1.0074	4.60319	1.0193	5.15761	1.0190	5.09787
4250	1.0	0.9947	4.67993	0.9980	4.67964	1.0046	4.67839	1.0074	4.67864	1.0067	4.68711	1.0153	5.04989
4500	1.0	0.9944	4.75176	0.9981	4.75033	1.0044	4.74973	1.0073	4.74970	1.0078	4.75097	1.0075	4.75112
4750	1.0	0.9941	4.81947	0.9985	4.81814	1.0046	4.81692	1.0069	4.81882	1.0070	4.81943	1.0071	4.81955
5000	1.0	0.9945	4.88441	0.9985	4.88207	1.0049	4.88201	1.0067	4.88369	1.0067	4.88503	1.0067	4.88525
5250	1.0	0.9952	4.94464	0.9986	4.94270	1.0042	4.94424	1.0055	4.94662	1.0057	4.94798	1.0060	4.94819
5500	1.0	0.9950	5.00216	0.9988	5.00136	1.0036	5.00362	1.0049	5.00650	1.0052	5.00817	1.0055	5.00831
5750	1.0	0.9948	5.06358	0.9984	5.05770	1.0032	5.06060	1.0040	5.06406	1.0044	5.06547	1.0044	5.06585
6000	1.0	0.9945	5.11890	0.9973	5.12022	1.0007	5.12490	1.0023	5.12814	1.0025	5.12313	1.0025	5.12261
6250	1.0	0.9939	5.17333	0.9961	5.17565	0.9994	5.18060	1.0008	5.18379	1.0008	5.18547	1.0011	5.18575
6500	1.0	0.9936	5.22647	0.9954	5.22945	0.9986	5.23480	0.9993	5.23800	0.9997	5.23945	0.9995	5.23994
6750	1.0	0.9933	5.27839	0.9950	5.28189	0.9977	5.28754	0.9982	5.29084	0.9984	5.29219	0.9987	5.29243
7000	1.0	0.9931	5.32864	0.9944	5.33263	0.9968	5.33829	0.9972	5.34139	0.9975	5.34285	0.9976	5.34311
3500	2.0	0.9998	4.42533	1.0031	4.43420	1.0066	4.44607	1.0096	4.46479	1.0240	5.11305	1.0231	5.05232
3750	2.0	0.9988	4.51696	1.0016	4.52315	1.0061	4.52602	1.0083	4.53136	1.0199	5.07210	1.0190	4.98957
4000	2.0	0.9971	4.60198	1.0001	4.60521	1.0056	4.60555	1.0079	4.60728	1.0086	4.61120	1.0091	4.61300
4250	2.0	0.9956	4.67997	0.9993	4.68087	1.0050	4.68084	1.0076	4.68248	1.0086	4.68497	1.0082	4.68612
4500	2.0	0.9952	4.75207	0.9988	4.75191	1.0044	4.75252	1.0078	4.75424	1.0079	4.75586	1.0082	4.75593
4750	2.0	0.9948	4.82019	0.9986	4.81920	1.0047	4.81935	1.0072	4.82218	1.0080	4.82302	1.0078	4.82340
5000	2.0	0.9950	4.88469	0.9989	4.88313	1.0051	4.88398	1.0070	4.88632	1.0074	4.88783	1.0071	4.88856
5250	2.0	0.9950	4.94564	0.9995	4.94437	1.0052	4.94517	1.0065	4.94825	1.0067	4.95003	1.0066	4.95054
5500	2.0	0.9955	5.00359	0.9995	5.00214	1.0046	5.00402	1.0063	5.00737	1.0066	5.00916	1.0064	5.00963
5750	2.0	0.9954	5.05822	0.9992	5.05752	1.0043	5.06062	1.0050	5.06436	1.0052	5.06617	1.0050	5.06660
6000	2.0	0.9953	5.11042	0.9987	5.11112	1.0032	5.11521	1.0040	5.11896	1.0046	5.12050	1.0045	5.12096
6250	2.0	0.9945	5.16999	0.9980	5.16360	1.0018	5.16837	1.0031	5.17173	1.0033	5.17350	1.0031	5.17391
6500	2.0	0.9941	5.22146	0.9961	5.22437	0.9998	5.23000	1.0007	5.23372	1.0011	5.22597	1.0011	5.22834
6750	2.0	0.9933	5.27227	0.9950	5.27539	0.9983	5.28112	0.9994	5.28438	0.9992	5.28613	0.9995	5.28638
7000	2.0	0.9923	5.32181	0.9941	5.32526	0.9967	5.33092	0.9973	5.33412	0.9976	5.33545	0.9979	5.33568
3500	3.0	1.0021	4.42213	1.0042	4.43369	1.0099	4.46446	1.0106	4.47431	1.0220	4.99945	1.0209	4.91991
3750	3.0	1.0000	4.51390	1.0034	4.52069	1.0075	4.53529	1.0094	4.54596	1.0106	4.54900	1.0105	4.54992
4000	3.0	0.9987	4.59940	1.0021	4.60357	1.0061	4.60656	1.0079	4.61339	1.0094	4.62013	1.0103	4.62211
4250	3.0	0.9971	4.67846	1.0005	4.68050	1.0053	4.68180	1.0075	4.68427	1.0085	4.68986	1.0092	4.69116
4500	3.0	0.9958	4.75153	0.9999	4.75209	1.0052	4.75296	1.0075	4.75602	1.0087	4.75800	1.0081	4.75900
4750	3.0	0.9953	4.81993	0.9993	4.81989	1.0051	4.82103	1.0076	4.82362	1.0082	4.82517	1.0079	4.82579
5000	3.0	0.9948	4.88470	0.9995	4.88385	1.0050	4.88527	1.0072	4.88775	1.0080	4.88916	1.0078	4.88989
5250	3.0	0.9953	4.94590	0.9994	4.94559	1.0053	4.94604	1.0073	4.94865	1.0074	4.95109	1.0078	4.95150
5500	3.0	0.9957	5.00461	0.9996	5.00336	1.0055	5.00450	1.0069	5.00809	1.0072	5.01022	1.0073	5.01069
5750	3.0	0.9956	5.05940	0.9996	5.05849	1.0051	5.06092	1.0062	5.06496	1.0065	5.06700	1.0066	5.06745
6000	3.0	0.9960	5.11158	0.9998	5.11139	1.0046	5.11537	1.0058	5.11931	1.0059	5.12131	1.0060	5.12176
6250	3.0	0.9959	5.16213	0.9999	5.16263	1.0037	5.16789	1.0049	5.17170	1.0051	5.17362	1.0050	5.17404
6500	3.0	0.9961	5.21122	0.9992	5.21296	1.0026	5.21860	1.0036	5.22229	1.0040	5.22396	1.0041	5.22436
6750	3.0	0.9960	5.26760	0.9983	5.26248	1.0016	5.26782	1.0026	5.27123	1.0026	5.27283	1.0026	5.27324
7000	3.0	0.9957	5.31547	0.9978	5.31901	1.0005	5.32567	1.0014	5.32951	1.0010	5.32118	1.0011	5.32229

$(V-K) = 1.4-3.6$. However, in the borders of the colour range of our calibration differences increase. The discrepancies at the cooler edge of the temperature scale point are probably connected with the limitations of Kurucz's (1993) models under $4500-4000$ K, however the reason for the discrepancy at the hotter edge is unclear.

Blackwell and Lynas-Gray 1998 (BL98)

This work presents a re-analysis of the results of Blackwell & Petford (1991) by using the same techniques. In Fig. 3c, we show the ratio of our bolometric flux to that of BL98 versus temperature for 50 giants common to both works. The mean difference is 1.4% (BL98 fluxes greater) with a dispersion of 1.7%. No appreciable trend with temperature is observed in the range $4000-8000$ K. The offset is probably related to the different absolute flux calibrations adopted.

Flower (1996; F96)

This study provides a thorough analysis of the bolometric correction based on measurements of 335 stars compiled from the literature. For 37 giants common with our sample (mainly Population I stars), we have transformed the BC(V) provided in Table 3 of F96 to BC(K) adopting the following parameters for the Sun: BC$_\odot(V) = -0.12$ and $(V-K)_\odot = 1.524$. From the comparison, two main

Table 5. Bolometric correction to $K_{\rm TCS}$ magnitude versus $(V-K)_{\rm TCS}$

$(V-K)$	BC(K)							
	[Fe/H] =0.00		[Fe/H] =−1.0		[Fe/H] =−2.0		[Fe/H] =−3.0	
	dwarfs	giants	dwarfs	giants	dwarfs	giants	dwarfs	giants
0.800	0.754	0.795	(0.710)	(0.736)	—	—	—	—
0.900	0.849	0.889	0.805	0.833	—	—	—	—
1.000	0.943	0.981	0.899	0.928	—	—	—	—
1.100	1.037	1.071	0.993	1.021	(0.950)	(0.970)	(0.910)	(0.919)
1.200	1.129	1.159	1.085	1.111	1.043	1.063	1.003	1.015
1.300	1.219	1.244	1.176	1.199	1.135	1.154	1.095	1.109
1.400	1.307	1.327	1.265	1.284	1.224	1.242	1.185	1.200
1.500	1.392	1.407	1.352	1.368	1.312	1.328	1.275	1.289
1.600	1.475	1.486	1.436	1.449	1.398	1.412	1.362	1.376
1.700	1.553	1.562	1.517	1.528	1.483	1.494	1.450	1.460
1.800	1.625	1.635	1.594	1.604	1.563	1.573	1.534	1.542
1.900	1.695	1.707	1.667	1.678	1.641	1.650	1.615	1.622
2.000	1.761	1.778	1.738	1.755	1.716	1.732	1.694	1.710
2.100	1.824	1.843	1.806	1.824	1.789	1.805	1.771	1.786
2.200	1.885	1.903	1.872	1.885	1.860	1.868	—	1.850
2.300	1.941	1.962	1.937	1.945	1.932	1.928	—	1.911
2.400	1.995	2.018	2.000	2.003	1.995	1.987	—	1.971
2.500	2.046	2.073	(2.046)	2.058	(2.046)	2.043	—	2.029
2.600	2.093	2.126	—	2.112	—	2.098	—	2.084
2.700	2.139	2.176	—	2.163	—	2.151	—	2.138
2.800	2.183	2.225	—	2.213	—	2.201	—	2.189
2.900	2.225	2.271	—	2.260	—	2.250	—	2.239
3.000	(2.268)	2.316	—	2.306	—	2.296	—	(2.287)
3.100	—	2.358	—	2.349	—	(2.341)	—	—
3.200	—	2.399	—	2.391	—	—	—	—
3.300	—	2.437	—	(2.430)	—	—	—	—
3.400	—	2.473	—	—	—	—	—	—
3.500	—	2.508	—	—	—	—	—	—
3.600	—	2.540	—	—	—	—	—	—
3.700	—	2.571	—	—	—	—	—	—
3.800	—	(2.599)	—	—	—	—	—	—

features can be observed in Fig. 4b. The differences show a conspicuous slope with colour. The probable reason for this trend is coupled with the different temperature scales adopted in both studies. Furthermore the scatter about the mean line of differences is slightly larger ($\approx 3\%$) than expected if one sums in quadrature the internal errors of both works. The explanation of this point, apart from the different temperature scales used implicity in the calculation, may be partly related to the inhomogeneity of the F96 sample and partly to the uncertainties introduced by the transformation from BC(V) to BC(K).

Bell & Gustaffson 1989 (BG89)

This study is based on a method similar to that applied here using instead 13-colour, UV and broad-band near-IR photometry. There are 21 common stars whose fluxes appear to be shifted 6% with a dispersion of 1.7% (Fig. 4c) from ours. This difference is probably connected with the absolute flux calibration and the photometric calibration of the 13-colour system. Notice that BG89 fluxes are also shifted $4-5\%$ with respect to those of BL98, so that the relative differences with our work are consistent.

In summary, the agreement of the bolometric fluxes derived here for solar metallicity stars is within the error-bars expected from the sources of uncertainty affecting the various methods: errors in the absolute calibrations adopted in the optical and IR ranges, differences in the atmosphere models grids. It is worth noting at this point that a 3% error on the bolometric flux implies a 1% error in the temperature derived by mean of the IRFM.

4.3. The reddening correction

A considerable number of the stars in the sample are distant from the solar neighbourhood ($D > 300$ pc),

Table 6. Temperatures derived for the field stars of the sample. Column 1: Identification. The stars are ordered in right ascension. Column 2: Metallicity. Column 3: Surface gravity. Column 4: Bolometric flux in 10^{-2} erg cm^{-2} s^{-1}. Column 5: Interstellar reddening. Column 6: Temperature derived in band J (units are K). Column 7: Error in T_J computed considering errors in $F_{\rm Bol}$, monochromatic fluxes, log(g) and [Fe/H]. Columns 8–9: The same as in Cols. 6–7 for temperature derived in band H. Columns 10–11: The same as in Cols. 6–7 for temperature derived in band K. Columns 12–13: The same as in Cols. 6–7 for temperature derived in band L'. Column 14: The weighted mean temperature derived from T_J, T_H, T_K and $T_{L'}$. Column 15: Mean error computed by considering linear transmission of errors from Cols. 7, 9, 11 and 13. Column 16. Number of temperatures considered in the average of Col. 14

ID	[Fe/H]	log(g)	$F_{\rm Bol}$	$E(B-V)$	T_J	ΔT_J	T_H	ΔT_H	T_K	ΔT_K	$T_{L'}$	$\Delta T_{L'}$	$T_{\rm mean}$	$\Delta T_{\rm mean}$	n
SAO166037	−1.66	2.00	7.286E-11	0.008	5387	113	5353	77	5327	71	—	—	5351	84	3
SAO147079	−1.38	0.00	4.436E-11	0.000	5054	82	4945	57	4933	56	—	—	4968	63	3
SAO166160	−1.12	2.00	4.592E-11	0.015	5273	117	5284	79	5244	66	—	—	5265	83	3
BS0080	−0.16	2.10	3.450E-09	0.000	4276	142	4182	46	4186	34	—	—	4184	39	2
BS0088	0.14	4.50	7.418E-10	0.000	5741	118	5765	98	5700	97	—	—	5735	103	3
SAO073973	−0.11	2.50	1.807E-10	0.020	7507	184	7484	152	7484	144	—	—	7491	158	3
SAO021465	−1.92	2.40	3.149E-10	0.065	4986	107	4978	72	5000	61	—	—	4990	66	2
BS0114	0.00	3.00	2.006E-09	0.000	6990	148	—	—	7006	113	6907	232	6979	200	3
SAO147321	−2.35	1.41	1.353E-10	0.000	4848	105	4869	63	4866	53	—	—	4867	58	2
SAO074086	−0.50	2.50	6.151E-10	0.000	4717	172	4797	70	4789	52	—	—	4792	60	2
HD3008	−1.85	1.50	7.439E-11	0.015	<3500	—	3923	70	4047	60	—	—	4047	60	1
SAO166375	−0.92	2.00	3.793E-11	0.010	5244	116	5239	75	5222	68	—	—	5233	82	3
BS0163	−0.70	2.40	5.772E-09	0.000	4837	104	4890	67	4889	54	4962	58	4914	59	3
HR0165	0.02	1.95	2.067E-08	0.000	4209	242	4333	68	4326	38	4332	65	4329	53	3
HR0168	−0.10	2.10	4.697E-08	0.000	4557	187	4591	70	4585	47	4568	70	4582	60	3
BS0219	−0.22	4.40	1.122E-08	0.000	5648	164	5842	94	5818	89	—	—	5790	107	3
SAO054175	−1.28	2.00	3.835E-10	0.045	4542	101	4535	49	4568	41	—	—	4553	45	2
BS0253	−0.25	1.75	5.055E-09	0.030	4602	130	4460	50	4447	40	—	—	4453	44	2
BD-20 0170	−1.90	2.00	2.469E-11	0.019	5035	118	5092	76	5119	59	—	—	5091	78	3
SAO036851	−0.80	2.00	6.291E-10	0.030	4996	146	4941	83	4946	61	—	—	4944	70	2
SAO147600	−0.93	2.30	2.840E-10	0.028	5043	122	5065	73	5082	53	—	—	5068	74	3
BS0316	−0.40	2.40	1.090E-09	0.000	4323	264	4436	86	4407	51	4408	21	4412	38	3
HD6833	−0.91	1.50	9.966E-10	0.065	4350	117	4358	57	4395	38	4476	79	4402	53	3
BS0337	0.00	1.60	1.227E-07	0.000	3687	214	3767	30	3786	21	3775	49	3783	29	2
BS0343	0.00	2.00	4.563E-09	0.000	7709	173	7818	154	7822	142	—	—	7787	155	3
HD7424	−0.54	4.00	2.731E-11	0.020	5686	159	5635	94	5585	—	—	82	5625	103	3
BS0402	−0.15	2.80	1.280E-08	0.000	4600	137	4705	61	4668	46	4700	54	4689	53	3
SAO092437	−1.60	1.50	2.040E-10	0.040	4460	123	4527	50	4542	41	—	—	4535	45	2
SAO167076	−1.50	2.00	9.157E-11	0.010	4827	110	4828	69	4842	54	—	—	4836	61	2
BS0434	−0.39	1.90	6.326E-09	0.000	4023	142	4031	34	4054	26	4068	183	4046	41	3
BS0448	0.09	3.84	1.319E-09	0.000	5770	119	5797	89	5749	88	5860	218	5783	112	4
BS0464	−0.03	2.00	1.565E-08	0.000	4281	148	4386	61	4354	35	4348	35	4359	41	3
BS0489	−0.30	1.50	8.598E-09	0.000	3976	177	4104	51	4118	30	4116	36	4114	37	3
SAO092437	−1.60	1.50	2.040E-10	0.040	4460	123	4527	50	4542	41	—	—	4535	45	2
SAO167076	−1.50	2.00	9.157E-11	0.010	4827	110	4828	69	4842	54	—	—	4836	61	2
BS0434	−0.39	1.90	6.326E-09	0.000	4023	142	4031	34	4054	26	4068	183	4046	41	3
BS0448	0.09	3.84	1.319E-09	0.000	5770	119	5797	89	5749	88	5860	218	5783	112	4
BS0464	−0.03	2.00	1.565E-08	0.000	4281	148	4386	61	4354	35	4348	35	4359	41	3
BD-18 0271	−1.92	0.00	5.807E-11	0.005	4333	98	4269	56	4283	38	—	—	4277	45	2
BS0489	−0.30	1.50	8.598E-09	0.000	3976	177	4104	51	4118	30	4116	36	4114	37	3
BS0557	−0.50	2.50	1.935E-09	0.000	4569	120	4643	65	4633	49	4673	69	4648	60	3
HR0603	−0.25	1.05	6.651E-08	0.010	4273	230	4275	67	4277	34	4279	63	4277	50	3
HR0617	−0.20	2.50	6.252E-08	0.000	4477	194	4505	71	4460	48	4519	70	4490	61	3
BS0672	−0.01	4.05	1.539E-09	0.000	5856	153	5919	92	5875	83	5991	154	5906	111	4
BD-22 0395	−2.00	1.75	2.104E-11	0.000	4813	106	4817	66	4813	52	—	—	4815	58	2
SAO167829	0.00	2.00	3.877E-10	0.010	4818	122	4868	64	4840	71	—	—	4855	67	2
BS0731	−0.43	2.10	1.157E-09	0.025	4801	112	4788	62	4787	45	4913	92	4815	61	3
BD-10 548	−1.07	2.00	2.221E-11	0.000	4921	121	4904	66	4900	54	—	—	4902	59	2
BS0874	0.07	2.80	1.027E-08	0.000	4614	144	4628	56	4603	43	4596	48	4608	48	3
BS0911	0.00	1.23	9.943E-08	0.000	3547	166	3628	42	3703	22	3709	185	3704	39	2
BS0941	0.10	3.10	9.661E-09	0.000	4799	105	4899	60	4864	54	4875	78	4879	62	3
SAO148896	0.00	2.00	3.870E-10	0.045	4392	145	4318	44	4313	32	—	—	4315	37	2
HD21581	−1.70	2.00	1.231E-10	0.045	4877	122	4866	70	4874	53	—	—	4870	60	2
SAO130653	0.11	2.00	5.481E-10	0.000	4850	95	4789	62	4775	50	—	—	4781	55	2
BS1132	−0.50	1.75	1.277E-09	0.030	4761	113	4812	72	4783	46	4814	113	4798	67	3

Table 6. continued

ID	[Fe/H]	log(g)	$F_{\rm Bol}$	$E(B-V)$	T_J	ΔT_J	T_H	ΔT_H	T_K	ΔT_K	$T_{L'}$	$\Delta T_{L'}$	$T_{\rm mean}$	$\Delta T_{\rm mean}$	n
SAO111430	−0.90	1.30	1.092E-09	0.055	4251	131	4243	50	4289	32	4284	152	4273	52	3
SAO076423	−1.23	2.00	1.907E-10	0.070	5381	116	5406	76	5395	73	—	—	5396	85	3
SAO149407	−1.64	1.20	4.424E-10	0.001	4319	109	4302	47	4337	36	—	—	4322	41	2
SAO111667	−1.94	0.80	1.452E-10	0.100	4064	181	4141	57	4218	40	—	—	4186	47	2
BS1318	0.20	2.70	4.489E-09	0.020	4675	258	4625	136	4549	46	4592	58	4577	65	3
SAO094040	0.10	2.00	2.646E-10	0.010	5793	151	5710	108	5685	101	—	—	5722	116	3
HR1457	−0.05	1.75	3.247E-07	0.000	3723	272	3806	62	3856	26	3888	54	3866	35	2
SAO149791	−1.79	1.50	2.985E-10	0.049	<3500	—	3908	65	4020	87	—	—	4020	87	1
BS1517	0.00	2.00	1.752E-09	0.060	4553	142	4560	48	4541	39	—	—	4550	43	2
BS1726	−0.35	2.15	7.203E-09	0.000	4071	147	4170	61	4208	40	—	—	4193	48	2
BS1805	−0.18	1.60	4.708E-09	0.020	4075	203	4167	48	4192	34	4202	86	4185	48	3
BS1907	−0.54	2.50	8.193E-09	0.000	4643	134	4667	68	4659	49	4741	44	4693	52	3
BS2002	−0.06	2.50	4.064E-09	0.030	4826	111	4825	52	4784	45	4892	48	4833	48	3
BS2012	−0.10	2.25	9.515E-09	0.000	4572	122	4601	48	4574	40	4637	42	4604	43	3
BS2035	-0.62	2.75	1.087E-08	0.000	4583	140	4586	67	4592	44	4617	55	4599	54	3
BS2065	−0.43	0.80	4.390E-09	0.050	3748	286	3750	65	3873	21	3906	64	3881	32	2
HD43039	−0.31	2.50	6.492E-09	0.000	4603	183	4668	77	4661	53	—	—	4664	63	2
HD44007	−1.63	2.15	2.297E-10	0.050	4898	151	4867	80	4840	57	—	—	4851	67	2
BS2286	0.11	1.14	1.113E-07	0.000	3597	186	<3500	—	3628	14	3644	65	3631	23	2
BS2319	0.00	2.00	1.256E-09	0.025	4298	149	4301	45	4300	33	—	—	4300	38	2
HD45282	−1.40	3.30	1.952E-10	0.020	5285	152	5291	86	5229	77	—	—	5264	96	3
BS2459	−0.03	1.75	6.094E-09	0.010	3769	255	3975	62	3975	87	—	—	3975	87	1
BS2557	0.30	3.40	1.206E-09	0.030	3926	201	4827	94	4909	82	—	—	4871	88	2
BS2560	0.05	3.10	5.500E-09	0.000	5251	229	5136	96	5062	58	5048	70	5092	86	4
BS2649	0.00	2.00	4.707E-09	0.030	3908	510	4146	227	4165	70	—	—	4161	107	2
SAO152627	0.00	2.00	5.122E-10	0.000	3744	228	3800	44	3856	69	—	—	3856	69	1
SAO152644	0.00	2.00	5.937E-11	0.000	6342	208	6305	98	6317	92	—	—	6317	116	3
BS2880	0.19	3.10	2.156E-09	0.040	7432	194	7409	167	7441	159	7482	102	7447	147	4
BS2927	0.44	3.21	2.182E-09	0.000	6386	204	6372	187	6390	188	6337	53	6358	116	4
BS2938	0.00	1.00	7.447E-09	0.008	3861	320	3827	67	3822	65	—	—	3822	65	1
BS2985	−0.04	2.60	1.160E-08	0.000	4983	127	5026	55	4974	55	5004	58	5001	56	3
BS2990	0.00	2.50	1.149E-07	0.000	4867	169	4858	73	4819	53	4904	85	4854	68	3
BS3003	−0.27	1.67	6.955E-09	0.000	4008	254	3967	75	3961	99	—	—	3961	99	1
BS3304	0.00	2.00	3.078E-09	0.000	3985	217	4104	56	4096	48	—	—	4100	52	2
BS3305	0.00	1.00	3.208E-09	0.020	4059	406	4001	107	3994	56	—	—	3996	74	2
BS3323	−0.12	2.50	1.355E-08	0.000	5125	164	5172	87	5123	58	5124	94	5136	88	4
BS3357	0.00	1.00	5.876E-09	0.005	3713	312	3810	66	3803	60	—	—	3803	60	1
BS3369	0.03	2.10	9.660E-10	0.000	4686	186	4759	74	4752	53	4786	78	4764	66	3
BS3403	−0.23	2.00	5.944E-09	0.000	4251	228	4385	73	4388	42	—	—	4387	53	2
HD73394	−1.40	1.30	3.162E-10	0.060	4662	158	4559	74	4559	50	4556	55	4558	58	3
BS3475	−0.05	2.15	7.890E-09	0.000	4950	142	4928	69	4886	54	4925	58	4911	60	3
BS3547	−0.04	2.50	1.858E-08	0.000	4841	169	—	—	4841	56	4741	81	4800	66	2
BS3550	0.00	1.00	3.489E-09	0.020	4439	213	4288	66	4186	57	—	—	4233	61	2
BS3660	0.00	1.00	5.414E-09	0.000	4127	195	3891	39	3876	40	—	—	3876	40	1
BS3664	−0.85	2.20	1.326E-09	0.015	5049	136	5013	65	5033	54	5087	43	5050	62	4
BS3705	0.00	1.53	3.974E-08	0.000	3798	248	3781	44	3854	25	3900	131	3861	42	2
HD81192	−0.64	2.60	8.846E-10	0.010	4698	107	4687	56	4701	49	4775	141	4707	66	3
HD82590	−1.85	2.75	5.365E-11	0.040	6015	134	5991	94	6013	93	—	—	6005	104	3
HD83212	−1.47	1.25	2.013E-10	0.025	4434	130	4431	55	4473	42	—	—	4455	48	2
BS3905	0.16	2.40	1.082E-08	0.000	4401	202	4529	75	4492	51	4483	75	4500	65	3
HD87140	−1.86	2.65	7.949E-11	0.000	4933	164	5012	91	5034	70	—	—	5024	79	3
BS3994	0.10	2.83	1.158E-08	0.000	4850	161	4918	83	4869	61	4810	80	4865	73	3
HD88609	−2.60	1.30	1.386E-10	0.000	4632	153	4582	96	4612	60	—	—	4600	74	2
BS4030	−0.03	4.00	1.104E-09	0.000	5604	129	5641	80	5657	95	—	—	5637	97	3
BS4042	0.09	3.76	1.961E-09	0.000	6976	184	6981	143	7012	137	7102	65	7040	114	4
HD093529	−1.70	2.00	7.705E-11	0.065	4850	98	4812	62	4835	52	—	—	4825	57	2
BS4246	−0.10	2.30	4.304E-09	0.000	4270	216	4250	70	4222	40	4227	66	4231	55	3
BS4247	−0.20	2.80	1.051E-08	0.000	4614	123	4648	59	4636	47	4646	57	4643	54	3
BS4291	−0.18	2.75	4.510E-09	0.000	4468	193	4497	72	4486	46	4491	72	4490	61	3
BS4309	0.00	3.00	1.007E-09	0.010	7832	161	7816	147	7820	134	—	—	7822	147	3

Table 6. continued

ID	[Fe/H]	log(g)	$F_{\rm Bol}$	$E(B-V)$	T_J	ΔT_J	T_H	ΔT_H	T_K	ΔT_K	$T_{L'}$	$\Delta T_{L'}$	$T_{\rm mean}$	$\Delta T_{\rm mean}$	n
BS4336	0.00	2.00	5.330E-09	0.000	<3500	—	3568	62	3655	78	3646	65	3650	70	2
BS4382	−0.40	2.50	1.450E-08	0.000	4476	117	—	—	4504	39	4423	48	4468	43	2
BS4392	−0.03	2.30	3.238E-09	0.000	4915	122	4905	116	4854	50	4880	88	4872	75	3
BD+04 2466	−1.88	1.80	2.013E-11	0.016	5067	151	5094	74	5123	58	—	—	5103	80	3
BS4432	−0.39	1.67	7.972E-09	0.000	3629	187	3792	71	3920	58	3876	32	3891	41	2
BS4452	−0.40	2.50	1.019E-09	0.020	4670	121	4680	62	4687	48	4737	51	4702	53	3
BS4474	−0.33	2.00	1.226E-09	0.030	4885	113	4883	57	4883	50	4827	138	4874	67	3
BD+22 2411	−1.95	1.25	4.144E-11	0.018	4354	186	4346	77	4388	47	—	—	4372	58	2
BD-01 2582	−2.20	1.20	4.581E-11	0.005	5177	163	5151	95	5134	71	—	—	5148	98	3
BS4518	−0.50	1.60	1.355E-08	0.000	4339	117	—	—	4374	36	4319	40	4348	38	2
HD103545	−2.30	2.00	6.137E-11	0.000	4655	156	4659	89	4671	59	—	—	4666	71	2
BD+09 2574	−2.40	2.00	2.077E-11	0.000	4855	145	4825	82	4875	63	—	—	4853	71	2
BS4608	−0.38	2.75	7.399E-09	0.000	4789	105	4834	53	4831	48	4807	51	4824	51	3
HD105546	−1.40	2.40	1.093E-10	0.000	5227	153	5203	91	5165	66	—	—	5190	92	3
HD106373	−2.48	2.80	9.294E-11	0.060	6088	186	6076	114	6111	108	—	—	6093	128	3
BS4695	−0.40	2.40	4.297E-09	0.000	4328	112	4364	46	4377	37	4364	43	4369	42	3
HD107328	−0.47	2.20	4.274E-09	0.000	4317	208	4418	76	4384	43	—	—	4396	55	2
BS4716	−0.25	2.30	3.684E-09	0.000	5017	113	5053	60	5033	59	5010	106	5033	77	4
HD108317	−2.30	2.40	1.891E-10	0.000	5220	117	5248	78	5230	75	—	—	5234	86	3
HD108577	−2.50	2.00	4.936E-11	0.020	4987	113	5008	75	5031	64	—	—	5020	69	2
HD110184	−2.26	0.90	2.157E-10	0.000	4187	155	4213	64	4273	39	—	—	4250	48	2
HD110281	0.00	2.00	1.170E-10	0.015	3668	204	3890	72	3950	54	—	—	3950	54	1
BS4883	0.11	2.50	2.869E-09	0.000	5597	87	5567	86	5581	95	5565	50	5589	76	4
BD+73 566	−1.32	2.00	5.413E-11	0.000	5642	161	5616	96	5626	90	—	—	5626	108	3
BS4902	0.00	2.00	1.754E-08	0.020	3638	214	3510	66	3630	54	3586	50	3607	52	2
BD+10 2495	−1.83	2.00	4.184E-11	0.003	4946	119	4916	69	4964	74	—	—	4939	71	2
BS4932	0.02	2.75	2.251E-08	0.000	5089	103	5067	55	5031	54	5004	61	5043	64	4
BS4981	−0.15	4.00	2.465E-09	0.000	6259	133	6250	111	6255	95	6182	145	6240	118	4
HD115444	−2.70	1.85	9.165E-11	0.000	4731	102	4703	71	4735	53	—	—	4721	61	2
BS5017	0.30	3.75	3.091E-09	0.000	7117	187	7157	170	7178	160	7096	217	7141	181	4
SAO028774	0.00	2.00	3.738E-10	0.020	4648	230	4575	63	4584	45	—	—	4580	52	2
BS5102	−0.50	2.25	1.317E-09	0.020	4706	135	4720	60	4712	47	4683	64	4706	56	3
BD+18 2757	−2.60	2.00	4.070E-11	0.000	4823	94	4841	64	4864	56	—	—	4853	60	2
HD119516	−2.50	2.50	6.983E-11	0.000	5448	128	5487	86	5483	83	—	—	5476	95	3
HD121135	−1.70	2.00	6.025E-11	0.011	4942	103	4927	67	4940	60	—	—	4934	63	2
BS5263	0.00	3.00	8.246E-10	0.015	7663	186	7676	159	7673	148	—	—	7671	163	3
HD122563	−2.62	1.60	1.248E-09	0.000	4542	96	4534	85	4589	55	4578	51	4572	61	3
SAO063927	0.00	2.00	3.435E-11	0.000	5772	132	5898	89	5917	86	—	—	5867	99	3
SAO158392	0.00	2.50	6.437E-11	0.020	5940	131	5898	89	5909	89	—	—	5913	100	3
BS5301	0.00	0.93	1.217E-08	0.000	<3500	—	3500	49	3669	67	3679	108	3672	82	2
HD124358	−2.20	1.75	6.484E-11	0.042	4718	100	4668	71	4703	55	—	—	4688	62	2
BD+09 2860	−2.60	2.00	1.470E-11	0.004	5391	281	5278	78	5260	83	—	—	5285	106	3
HR5340	−0.50	1.75	4.830E-07	0.000	4187	225	4166	79	4247	38	4263	64	4233	55	3
BD+08 2856	−2.05	1.00	3.934E-11	0.005	4541	94	4506	54	4520	43	—	—	4514	48	2
HD126587	−2.70	2.00	9.370E-11	0.070	4790	92	4776	65	4809	52	—	—	4794	58	2
HD126778	0.11	2.00	1.815E-10	0.000	4859	153	4779	80	4778	56	—	—	4778	66	2
BD+18 2890	−1.61	2.00	3.954E-11	0.030	5063	108	5049	68	5060	61	—	—	5057	74	3
BS5429	−0.30	1.80	1.638E-08	0.000	4307	175	4267	71	4275	34	4267	77	4271	53	3
HD128279	−2.22	3.00	2.185E-10	0.050	5274	157	5282	94	5305	82	—	—	5290	103	3
BS5480	−0.22	2.00	3.729E-09	0.000	4872	106	4880	54	4831	47	4854	87	4854	58	3
BS5535	−0.38	2.65	3.657E-09	0.000	4672	119	4720	56	4713	48	4709	93	4715	61	3
HD130952	−0.38	2.50	3.761E-09	0.010	4623	178	4702	78	4713	55	—	—	4708	65	2
BD+30 2611	−1.40	1.00	1.048E-10	0.005	4258	209	4141	78	4244	40	—	—	4209	53	2
HD135722	−0.43	2.60	1.361E-08	0.000	4644	177	4776	72	4763	52	—	—	4768	60	2
BS5681	−0.43	2.50	1.342E-08	0.000	4778	103	—	—	4794	49	4802	49	4798	49	2
BS5694	−0.13	3.95	2.455E-09	0.000	6058	124	6067	86	6050	89	5964	104	6036	99	4
BS5709	−0.38	2.70	2.194E-09	0.000	4627	177	4692	56	4680	48	4624	170	4677	67	3
BS5787	−0.44	2.80	9.706E-09	0.010	4651	138	4732	55	4717	47	4686	47	4711	49	3
BS5802	−0.13	3.00	2.474E-09	0.000	4946	124	4974	62	4950	56	4953	54	4958	57	3
BS5804	0.00	2.50	1.053E-09	0.000	6661	122	6670	105	6655	102	—	—	6662	109	3

Table 6. continued

ID	[Fe/H]	log(g)	$F_{\rm Bol}$	$E(B-V)$	T_J	ΔT_J	T_H	ΔT_H	T_K	ΔT_K	$T_{L'}$	$\Delta T_{L'}$	$T_{\rm mean}$	$\Delta T_{\rm mean}$	n
BS5823	−0.55	3.20	2.581E-09	0.013	4889	118	4895	56	4890	52	4893	88	4893	62	3
BS5824	−0.10	2.30	5.166E-09	0.070	4334	130	4410	52	4403	40	4317	123	4392	57	3
HD141531	−1.57	1.00	9.446E-11	0.016	4874	144	4503	72	4433	49	—	—	4461	58	2
BS5889	−0.32	3.10	4.200E-09	0.000	5143	118	5187	70	5138	52	5252	69	5180	71	4
BD+05 3098	−2.60	2.00	2.284E-11	0.038	4840	94	4866	68	4893	58	—	—	4881	63	2
BD+11 2998[a]	−1.15	2.50	6.275E-11	0.048	9098	217	7191	140	6966	128	—	—	7073	134	2
BD+09 3223	−2.30	2.00	7.166E-11	0.060	5395	122	5366	79	5342	73	—	—	5363	87	3
BS6189	−0.62	3.95	7.891E-10	0.010	6008	135	6014	86	6016	87	—	—	6013	98	3
BS6213	0.00	3.00	1.058E-09	0.000	6445	132	6449	101	6466	104	6519	84	6474	103	4
BS6220	−0.20	3.00	1.261E-08	0.000	4917	130	4966	83	4931	55	4933	93	4942	73	3
HD151937	0.00	2.00	1.079E-09	0.010	4268	231	4322	64	4254	47	—	—	4283	54	2
BS6279	0.00	3.00	1.801E-09	0.000	6893	128	6878	111	6888	105	—	—	6886	114	3
BS6394	−0.14	3.95	5.793E-10	0.010	6159	128	6169	89	6156	93	—	—	6162	101	3
BS6469	0.00	2.00	1.733E-09	0.000	5398	157	5314	81	5263	74	—	—	5309	93	3
BS6480	0.00	2.00	1.251E-09	0.000	7392	154	7399	140	7399	131	—	—	7397	141	3
BD+17 3248	−2.04	1.80	6.465E-11	0.055	5272	109	5235	75	5213	71	—	—	5236	82	3
BS6541	−0.24	3.95	1.415E-09	0.000	6090	161	6112	103	6084	98	—	—	6096	115	3
BS6594	−0.13	4.00	1.533E-09	0.000	6496	170	6500	116	6472	113	—	—	6488	128	3
BS6603	0.05	2.30	2.952E-08	0.000	4497	151	4546	55	4524	40	—	—	4533	46	2
HD161770	−2.12	2.50	5.004E-11	0.075	5291	157	5275	94	5278	80	—	—	5280	102	3
BS6644	0.04	2.80	3.604E-09	0.020	4457	240	4514	117	4520	74	—	—	4518	91	2
BS6688	−0.12	2.50	1.238E-08	0.000	4467	144	4487	56	4472	42	4457	55	4472	50	3
BS6698	0.09	2.60	1.494E-08	0.000	4868	135	4900	71	4852	55	4865	88	4871	69	3
HR6705	−0.25	1.50	8.058E-08	0.000	3758	283	3862	72	3955	33	3898	56	3934	42	2
BS6722	0.00	2.00	8.683E-10	0.000	5533	107	5490	73	5460	72	—	—	5490	81	3
HD165195	−2.20	1.50	7.960E-10	0.130	4084	134	4153	64	4251	50	4350	108	4237	67	3
BS6770	−0.15	2.95	4.614E-09	0.020	4925	163	5003	63	4966	55	4937	69	4969	62	3
SAO142126	−1.21	2.31	3.752E-10	0.274	4878	106	4934	66	5008	56	—	—	4974	61	2
BS6791	0.06	2.65	3.215E-09	0.010	5006	108	5003	65	4952	62	5025	70	4994	73	4
BS6795	0.00	2.00	1.302E-09	0.010	6697	163	6660	121	6636	115	—	—	6661	130	3
BS6797	−0.22	3.90	1.407E-09	0.010	6335	167	6312	108	6298	105	—	—	6312	121	3
BS6817	0.00	2.00	1.332E-09	0.000	4959	117	4939	62	4886	52	4956	138	4918	70	3
BS6847	0.00	2.00	8.128E-10	0.000	5789	109	5736	78	5721	79	—	—	5745	87	3
BS6853	−0.30	2.00	1.257E-09	0.010	4844	109	4767	64	4753	50	4861	84	4785	63	3
BS6869	−0.19	3.10	1.658E-08	0.000	4839	106	4845	55	4817	48	4848	60	4835	54	3
BS6895	−0.27	2.65	1.162E-08	0.000	4384	141	4434	64	4440	41	4409	46	4428	49	3
HD170737	−0.91	3.00	1.979E-10	0.035	5134	159	5060	82	5062	69	—	—	5075	91	3
BS6969	0.00	3.00	6.457E-10	0.010	7126	142	7115	126	7121	117	—	—	7120	128	3
BS6970	−0.07	2.90	2.858E-09	0.010	4913	129	4990	61	4958	55	4864	41	4928	51	3
BS6973	−0.09	2.10	1.324E-08	0.000	4233	270	4254	90	4266	50	4218	69	4248	66	3
HD171496	−1.12	1.50	2.087E-10	0.107	4281	128	4476	63	4491	43	—	—	4485	51	2
BS7044	0.00	3.00	1.278E-09	0.000	6613	185	6648	117	6685	107	—	—	6655	129	3
BS7046	−0.29	1.70	5.972E-09	0.060	3669	235	3758	83	3863	54	—	—	3863	54	1
BS7250	0.00	3.00	1.199E-09	0.000	8196	184	8203	182	8230	170	—	—	8210	178	3
HD175179	−0.75	2.00	7.401E-11	0.050	5673	161	5638	97	5713	92	—	—	5676	110	3
BS7120	−0.40	1.00	4.757E-09	0.020	4115	365	4266	57	4293	34	—	—	4283	43	2
HD175305	−1.45	2.50	4.516E-10	0.025	5063	152	5028	85	5042	66	—	—	5041	90	3
BS7196	0.00	2.00	1.033E-09	0.010	4863	145	4816	66	4789	49	4890	59	4829	57	3
BS7300	0.21	2.00	2.192E-09	0.040	4786	122	4802	80	4792	66	4924	70	4840	72	3
BS7317	−0.60	1.40	2.490E-09	0.040	3805	197	3892	66	3989	34	4038	55	4008	42	2
BS7322	−0.28	4.17	1.018E-09	0.000	6262	141	6248	91	6213	96	6458	132	6285	111	4
BS7328	−0.10	2.85	9.830E-09	0.000	4893	129	4953	64	4926	54	4968	68	4947	61	3
HD182762	−0.20	3.01	2.998E-09	0.010	4641	182	4810	69	4750	52	—	—	4776	59	2
BD+26 3578	−2.30	2.50	5.593E-11	0.035	6487	182	6378	125	6413	122	—	—	6419	138	3
SAO162774	−1.57	1.85	3.091E-10	0.050	5592	125	5595	76	5577	75	—	—	5587	87	3
BS7429	−0.06	2.50	6.539E-09	0.000	4448	136	4513	45	4460	43	4393	139	4473	57	3
SAO162942	0.00	2.00	9.750E-11	0.080	4558	194	4556	67	4554	45	—	—	4555	54	2
SAO162947	−2.63	0.95	1.031E-10	0.078	4640	148	4579	80	4611	55	—	—	4598	65	2
SAO163006	−1.87	0.75	4.979E-10	0.111	4357	181	4229	80	4292	41	—	—	4271	54	2
BS7569	0.06	2.00	9.517E-10	0.000	5699	118	5637	89	5623	80	—	—	5648	93	3

Table 6. continued

ID	[Fe/H]	log(g)	$F_{\rm Bol}$	$E(B-V)$	T_J	ΔT_J	T_H	ΔT_H	T_K	ΔT_K	$T_{L'}$	$\Delta T_{L'}$	$T_{\rm mean}$	$\Delta T_{\rm mean}$	n
BS7576	−0.05	1.80	4.194E-09	0.010	4263	180	4383	48	4356	36	4388	50	4374	44	3
BS7596	0.00	2.00	1.520E-09	0.030	7882	163	7987	165	7969	151	—	—	7946	159	3
BS7601	0.00	3.00	1.659E-09	0.020	9100	213	9405	272	9229	194	—	—	9232	222	3
BS7610	0.47	4.30	1.891E-09	0.000	8764	235	8971	269	8839	222	—	—	8853	240	3
BS7615	0.08	2.20	9.360E-09	0.000	4838	111	4804	58	4760	49	4840	74	4796	59	3
BD-18 5550	−2.90	1.10	9.676E-11	0.100	4622	101	4655	75	4677	54	—	—	4668	63	2
BS7633	0.00	2.00	7.090E-09	0.020	3884	223	3888	46	3920	52	—	—	3920	52	1
BS7635	0.00	2.00	2.792E-08	0.000	3713	229	3833	50	3883	48	3850	53	3867	50	2
BS7636	−1.57	2.00	1.563E-09	0.060	4398	137	4447	61	4507	42	4405	78	4464	57	3
BS7653	0.01	3.60	3.573E-09	0.015	7809	175	7824	149	7809	135	7749	290	7804	172	4
SAO069416	−0.42	2.00	7.972E-10	0.110	4714	151	4525	62	4564	43	4655	80	4574	58	3
BS7701	0.12	2.50	2.744E-09	0.000	4386	180	4478	79	4461	48	—	—	4467	60	2
SAO144233	0.00	2.00	1.215E-10	0.015	5795	109	5717	80	5714	80	—	—	5737	88	3
BS7742	0.00	2.00	2.947E-09	0.020	3953	218	3973	43	4011	54	—	—	4011	54	1
BS7754	0.05	3.00	1.169E-08	0.000	5014	103	4997	59	4948	56	4968	71	4978	68	4
BS7776	−0.78	2.00	1.904E-08	0.000	4960	100	4898	57	4876	51	4860	56	4878	55	3
BS7794	−0.03	3.20	2.470E-09	0.000	4817	141	4884	74	4826	58	4967	188	4869	83	3
SAO144547	−2.79	3.40	5.584E-11	0.060	5378	161	5381	102	5389	91	—	—	5384	111	3
BS7850	0.14	4.00	5.134E-09	0.010	7722	166	7744	157	7702	144	7966	192	7774	163	4
BD-17 6036	−2.60	1.75	2.416E-11	0.049	4942	99	4869	79	4853	56	—	—	4860	66	2
BS7919	0.00	2.00	1.759E-09	0.020	4541	121	4435	51	4433	43	4510	52	4457	48	3
BS7928	−0.20	3.50	4.172E-09	0.000	6837	141	6881	114	6906	112	7330	156	6877	121	3
BD-15 5781	−2.40	1.50	2.297E-11	0.027	3890	254	4297	62	4402	46	—	—	4357	53	2
BS7949	−0.10	2.80	3.567E-08	0.000	4777	123	4726	62	4724	50	4727	80	4725	62	3
BS7957	−0.13	3.20	1.366E-08	0.000	4885	118	4935	60	4885	52	—	—	4908	56	2
BS7995	−0.13	2.85	4.368E-09	0.000	5112	127	5161	72	5125	53	—	—	5135	74	3
BS8005	−0.36	1.65	4.575E-09	0.030	3753	267	3841	62	3920	58	—	—	3920	58	1
HD199191	−0.70	2.25	5.296E-10	0.040	4920	157	4783	72	4809	53	—	—	4798	61	2
BS8025	0.00	2.00	1.170E-09	0.000	6845	131	6773	105	6774	110	—	—	6794	114	3
BS8097	0.07	4.00	3.245E-09	0.000	7418	158	7414	138	7423	127	7531	454	7429	169	4
SAO089549	0.00	2.00	1.304E-09	0.060	4722	142	4783	52	4753	47	—	—	4767	49	2
SAO050693	0.00	2.00	7.320E-11	0.000	7134	146	7131	127	7126	120	—	—	7130	130	3
SAO145433	−1.78	1.30	1.903E-10	0.033	4706	111	4666	66	4677	53	—	—	4672	59	2
SAO033445	−0.50	3.75	1.357E-10	0.020	5765	197	5781	103	5788	97	—	—	5781	120	3
BD-03 5215	−1.57	2.30	2.833E-11	0.044	5501	114	5488	78	5475	87	—	—	5487	91	3
BS8255	−0.01	2.45	3.963E-09	0.000	4548	141	4633	50	4608	43	4576	76	4609	53	3
BS8287	0.00	2.00	3.143E-09	0.035	3977	204	4062	48	4084	29	4035	86	4069	45	3
BS8289	0.00	2.00	7.974E-09	0.000	3582	172	3601	50	3697	25	3632	112	3685	41	2
SAO164618	−1.59	1.70	1.500E-10	0.032	4694	119	4639	57	4653	48	—	—	4647	52	2
BD-09 5831	−2.00	2.00	2.800E-11	0.023	4597	99	4528	57	4568	43	—	—	4551	49	2
BS8354	−0.60	4.10	1.604E-09	0.000	6221	127	6216	96	6242	94	6312	83	6252	98	4
SAO051484	0.00	2.00	1.866E-10	0.010	6011	124	5947	94	5930	89	—	—	5958	100	3
BS8448	−0.50	2.00	1.065E-09	0.000	5258	135	5279	95	5198	86	5301	70	5261	91	4
BS8454	0.00	2.00	4.898E-09	0.000	6255	128	6195	114	6174	98	6224	131	6209	116	4
BS8551	−0.33	1.05	4.449E-09	0.000	4639	138	4567	53	4564	42	4662	78	4588	54	3
BS8562	−0.21	1.60	4.244E-09	0.020	3808	282	3809	97	3886	28	3882	73	3885	40	2
BS8568	0.00	2.00	1.130E-09	0.020	4745	177	4706	77	4670	54	—	—	4685	63	2
BS8607	0.00	3.00	7.587E-10	0.030	8256	181	8290	187	8233	162	—	—	8258	176	3
SAO191281	−2.20	2.50	6.834E-11	0.008	5728	137	5741	87	5713	89	—	—	5727	100	3
BS8632	−0.25	2.30	7.782E-09	0.020	4378	153	4283	75	4277	35	4325	63	4292	52	3
BS8649	−0.23	2.05	7.504E-09	0.030	3838	212	4040	39	4104	38	—	—	4072	38	2
HD215373	−0.02	2.80	2.940E-09	0.015	4922	172	4971	77	4887	59	—	—	4923	67	2
BS8665	−0.31	4.00	5.455E-09	0.000	6063	121	6078	84	6072	84	6141	131	6085	101	4
BS8666	0.00	2.00	1.130E-09	0.000	6726	136	6700	116	6708	108	—	—	6711	119	3
SAO146344	−2.20	1.50	3.069E-10	0.018	4496	105	4461	63	4504	45	—	—	4486	52	2
BS8710	0.00	2.00	1.491E-09	0.020	4344	171	4356	55	4347	35	—	—	4350	43	2
BS8775	−0.25	0.23	1.560E-07	0.000	<3500	—	<3500	—	3623	55	3577	44	3598	49	2
HD218502	−1.85	3.75	1.502E-10	0.030	6310	183	6282	120	6301	112	—	—	6296	132	3
SAO165532	0.00	2.00	3.037E-10	0.100	3932	185	4024	59	4082	41	—	—	4058	48	2
BS8825	−0.28	4.10	1.094E-09	0.000	6124	122	6127	90	6100	92	—	—	6116	99	3

Table 6. continued

ID	[Fe/H]	log(g)	$F_{\rm Bol}$	$E(B-V)$	T_J	ΔT_J	T_H	ΔT_H	T_K	ΔT_K	$T_{L'}$	$\Delta T_{L'}$	$T_{\rm mean}$	$\Delta T_{\rm mean}$	n
BS8834	0.00	2.00	1.796E-08	0.000	3498	164	3688	79	3762	51	—	—	3762	51	1
HD219615	−0.44	2.50	1.102E-08	0.000	4837	159	4828	72	4824	55	—	—	4826	62	2
BS8878	0.00	2.00	4.519E-09	0.000	4304	226	4228	73	4238	57	—	—	4234	64	2
BS8905	0.11	2.00	4.548E-09	0.000	5904	122	5853	97	5834	91	6201	137	5928	109	4
SAO191895	−1.59	1.80	3.669E-11	0.008	4462	112	4449	61	4478	43	—	—	4466	50	2
BS8916	−0.10	2.40	6.691E-09	0.000	4720	138	4714	63	4672	46	4727	86	4699	61	3
BS8923	−0.03	2.91	4.768E-09	0.000	5007	133	4998	61	4936	54	4943	95	4967	76	4
HD221170	−2.16	1.10	4.027E-10	0.060	4520	134	4416	80	4434	53	4332	150	4410	79	3
BS8930	0.00	2.00	2.892E-09	0.000	4697	130	4695	78	4646	51	4546	42	4615	53	3
BS8961	−0.60	2.80	1.089E-08	0.000	4560	105	4620	65	4589	46	4534	49	4578	52	3
BS9057	0.00	2.00	1.306E-09	0.050	5613	111	5511	75	5471	72	5518	53	5520	73	4
SAO105082	−1.10	0.50	5.782E-10	0.160	<3500	—	<3500	—	3654	70	<3500	—	3654	70	1
BD+54 1323	−1.40	2.30	5.657E-11	0.005	5186	116	5191	74	5182	68	—	—	5186	81	3
BD+52 1601	−1.50	2.05	1.037E-10	0.020	4924	97	4906	61	4915	54	—	—	4911	57	2
SAO024707	0.00	2.00	1.459E-10	0.000	4903	173	4964	78	4939	62	—	—	4950	69	2
BD+58 1218	−2.63	1.90	3.392E-11	0.000	4968	123	4984	85	4985	65	—	—	4985	74	2
SAO078681	0.00	2.00	3.883E-11	0.000	5718	165	6146	110	6280	101	—	—	6095	120	3
HD268518[b]	0.11	2.00	2.879E-10	0.060	5746	160	6035	110	5869	103	—	—	5899	120	3
SAO103301	0.00	2.00	1.642E-10	0.000	4802	124	4824	50	4780	45	—	—	4801	47	2

[a] BD+11 2998 probable misidentification in the program of near IR photometry.
[b] HD 268518 variable?

and consequently extinction corrections have to be applied. For this purpose, we have estimated $E(B-V)$ for each star in the sample in order to correct both the bolometric and monochromatic fluxes. Where the values of the estimated extinction were considered significant, the colours have been corrected according to the extinction law ($A_\lambda = f(A_V, \lambda)$) compiled by Landolt-Börnstein (1982). Two independent methods have been considered for assigning $E(B-V)$ to field stars. The first one is based on the work by Anthony–Twarog & Twarog (1994), which provide $E(b-y)$ obtained with the reddening maps of Burnstein & Heiles (1982). In this case, we have considered $E(B-V) = 1.37E(b-y)$ (Crawford 1975). The second one makes use of the extinction models for the galaxy compiled by Hakkila et al. (1997) and the distances calculated from Hipparcos parallaxes. The values obtained by Anthony–Twarog & Twarog (1994) are preferred for metal-poor giants, since the parallaxes of these stars are affected by errors which made the second method more uncertain.

As for the stars of globular clusters, we have adopted an average of the most reliable values quoted in literature, and, except for M 71, we have restricted our analysis to low reddening clusters.

In Tables 6 and 7 we present the reddening correction applied to the stars of the sample. It is worth noticing that a third of the field stars of the sample needed a reddening correction $E(B-V) \geq 0.02$ mag, and that ∼10% of them have $E(B-V) \geq 0.05$ mag.

The change in temperature induced by $E(B-V) = 0.05$ mag when applying the IRFM varies from 2.1% at 3500 K to 4.5% at 7500 K. The hotter the star the stronger the effect since the proportion of flux radiated in the visible/UV wavelength range is greater.

4.4. Metallicity and surface gravity

The effective temperature determination by means of Eq. (3) requires an estimate of the stellar metallicity and surface gravity. These parameters, however, need not be very accurate as mentioned in Sect. 3.1. In particular, it may be concluded that 0.5 dex and 0.3 dex uncertainties in log(g) and [Fe/H], respectively, are sufficient to obtain temperatures to an accuracy of $1-2\%$ (see Fig. 2). Therefore, as far as the surface gravity is concerned, it is enough to consider an average surface gravity according to the spectral type, although spectroscopic determinations of surface gravities have been adopted when available from literature.

A number of stars in the sample had their metal abundance determined from fine spectroscopic analysis included in the Catalogue of [Fe/H] determinations of Cayrel de Strobel et al. (1997) with a mean accuracy within 0.15 dex. We have preferred these determinations, but for stars lacking spectroscopic analysis, photometric metallicity calibrations based on Strömgren photometry (Anthony-Twarog & Twarog 1994), and on $\delta_{0.6}(U-B)$ index (Carney 1979), with accuracies oscillating between $0.20-030$ dex, were used.

The adopted gravities and metallicities are listed in Tables 6 and 7.

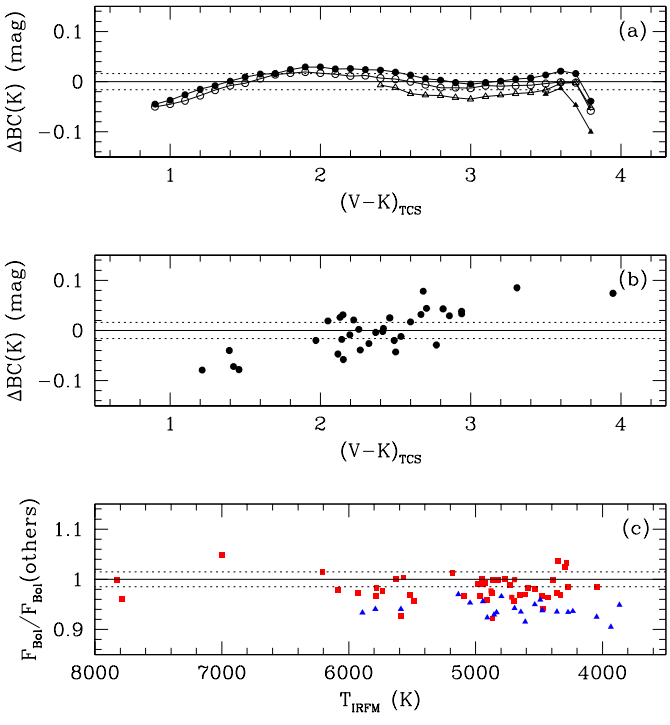

Fig. 4. a) Difference between the bolometric correction to $K_{\rm TCS}$ obtained here and those theoretically derived by Bessell et al. (1998): Solid circles: ATLAS9 Kurucz (1995) overshooting models, open circles: ATLAS9 Kurucz (1995) no overshooting models, solid triangles; NMARCS giant branch models of Plez et al. (1992), open triangles: NMARCS giant branch models of Plez (1995) **b)** Difference between the bolometric correction to $K_{\rm TCS}$ obtained here and that of Flower (1996); **c)** Ratios of the fluxes presented in this work to those obtained by Bell & Gustafsson (1989) (triangles), and Blackwell & Lynas-Gray (1998) (squares). Dotted lines show the internal error of our calibration (1.5%)

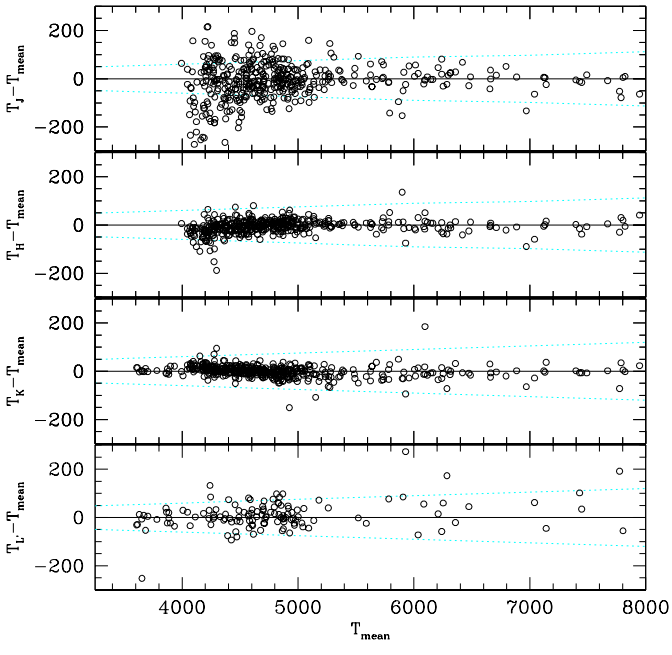

Fig. 5. Differences $T_J - T_{\rm mean}$, $T_H - T_{\rm mean}$, $T_K - T_{\rm mean}$ and $T_{L'} - T_{\rm mean}$ versus effective temperature (only temperatures obtained from more than one filter are displayed). The dotted lines show the region $|\Delta T| \leq 1.5\%$

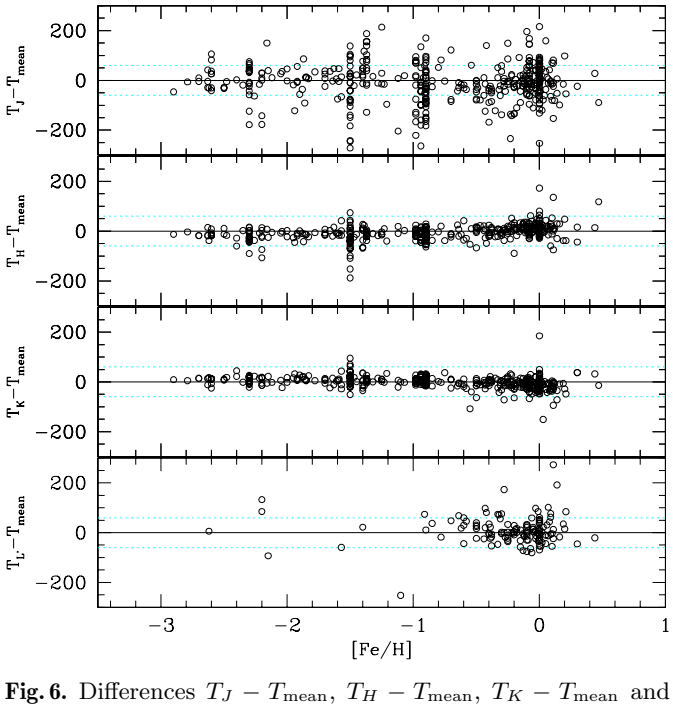

Fig. 6. Differences $T_J - T_{\rm mean}$, $T_H - T_{\rm mean}$, $T_K - T_{\rm mean}$ and $T_{L'} - T_{\rm mean}$ versus [Fe/H] (only temperatures obtained from more than one filter are displayed). The dotted lines show the region $|\Delta T| \leq 60$ K. The vertical accumulations correspond to the temperatures of the stars of the globular clusters contained in our sample

5. The determination of temperatures

According to the procedure described in the preceding sections, we have derived three (four) effective temperatures for each star in the sample by applying the IRFM at the IR wavelengths considered (Eq. 3). The individual values of T_J, T_H, T_K (and $T_{L'}$) derived with their corresponding errors, are listed in Tables 6 and 7.

The final temperature was derived as an average of T_J, T_H, T_K (and $T_{L'}$) weighted with the inverse of their errors:

$$\overline{T_{\rm IRFM}} = \frac{\sum\limits_{i=J,H,K,L} \dfrac{T_i}{\Delta T_i}}{\sum\limits_{i=J,H,K,L} \dfrac{1}{\Delta T_i}}. \qquad (6)$$

Table 7. Temperatures derived for the globular cluster stars of the sample. Column 1 Globular cluster. Column 2: Identification: M 3 nomenclature from Cohen et al. (1978) and Arribas & Martínez-Roger (1987); M 13, M 92 and M 67 nomenclature from Cohen et al. (1978); M 71 nomenclature from Frogel et al. (1979); 47 Tuc nomenclature from Frogel et al. (1981); NGC 288, NGC 1261, NGC 362 nomenclature from Frogel et al. (1983). Column 3: Metallicity. Column 4: Surface gravity. Column 5: Bolometric flux in 10^{-2} erg cm^{-2} s^{-1}. Column 6: Interstellar reddening. Column 7: Temperature derived in band J (units are K). Column 8: Error in T_J computed considering errors in $F_{\rm Bol}$, monochromatic fluxes, log(g) and [Fe/H]. Columns 9–10: The same as in Cols. 7–8 for temperature derived in band H. Columns 11–12: The same as in Cols. 7–8 for temperature derived in band K. Column 13: The weighted mean temperature derived from T_J, T_H and T_K. Column 14: Mean error computed by considering linear transmission of errors from Cols. 8, 10 and 12. Column 14. Number of temperatures considered in the average of Col. 13

GC	ID	[Fe/H]	log(g)	$F_{\rm Bol}$	$E(B-V)$	T_J	ΔT_J	T_H	ΔT_H	T_K	ΔT_K	$T_{\rm mean}$	$\Delta T_{\rm mean}$	n
M3	I21	−1.50	2.50	2.982E-12	0.00	4017	207	4024	84	4137	48	4096	61	2
M3	II18	−1.50	3.50	8.147E-13	0.00	4800	118	4689	85	4699	58	4695	69	2
M3	II46	−1.50	2.50	4.976E-12	0.00	3607	194	<3500	—	3927	52	3927	52	1
M3	III28	−1.50	2.50	3.947E-12	0.00	3843	240	3935	292	4073	43	4073	43	1
M3	III77	−1.50	2.75	2.215E-12	0.00	4269	151	4183	91	4224	44	4211	59	2
M3	IV25	−1.50	3.00	1.561E-12	0.00	4404	144	4327	72	4323	41	4324	52	2
M3	193	−1.50	3.50	4.270E-13	0.00	4749	128	4611	78	4678	57	4650	66	2
M3	216	−1.50	3.25	9.340E-13	0.00	4519	139	4452	85	4510	46	4490	60	2
M3	1397	−1.50	2.50	5.368E-12	0.00	3810	231	<3500	—	3916	53	3916	53	1
M3	AA	−1.50	2.50	4.993E-12	0.00	3966	208	3766	388	3953	50	3953	50	1
M3	BI	−1.50	3.00	8.872E-13	0.00	4422	150	4425	81	4487	50	4463	62	2
M3	26	−1.50	2.50	5.203E-12	0.00	3500	180	<3500	—	3877	57	3877	57	1
M3	33	−1.50	2.50	2.960E-12	0.00	3620	213	4057	72	4124	37	4101	49	2
M3	46	−1.50	2.75	9.325E-13	0.00	4416	148	4533	68	4408	47	4459	56	2
M3	53	−1.50	2.75	1.413E-12	0.00	3641	213	4109	89	4392	45	4297	60	2
M3	68	−1.50	2.75	9.867E-13	0.00	3787	240	4391	76	4334	41	4354	53	2
M3	72	−1.50	2.75	1.164E-12	0.00	3845	239	4124	90	4347	42	4276	57	2
M3	155	−1.50	3.00	7.694E-13	0.00	4570	133	4519	74	4579	49	4555	59	2
M3	311	−1.50	2.50	3.100E-12	0.00	4057	197	4153	82	4233	42	4206	56	2
M3	313	−1.50	3.00	1.168E-12	0.00	4374	153	4472	80	4538	46	4514	58	2
M3	428	−1.50	2.50	2.664E-12	0.00	4041	203	3997	131	4239	41	4239	41	1
M3	444	−1.50	2.50	2.208E-12	0.00	4189	166	4093	76	4203	43	4163	55	2
M3	464	−1.50	2.50	1.966E-12	0.00	3834	245	4082	75	4118	37	4106	50	2
M3	496	−1.50	2.50	2.377E-12	0.00	3713	234	4044	74	4216	43	4153	54	2
M3	525	−1.50	2.50	4.128E-12	0.00	3581	180	3937	285	3959	49	3959	49	1
M3	557	−1.50	2.50	2.453E-12	0.00	3783	250	3902	276	4162	40	4162	40	1
M3	567	−1.50	2.75	1.682E-12	0.00	4096	183	4180	93	4322	41	4279	57	2
M3	586	−1.50	2.50	5.014E-12	0.00	3946	209	<3500	—	3911	53	3911	53	1
M3	605	−1.50	2.75	8.909E-13	0.00	4282	157	4299	69	4409	46	4365	55	2
M3	617	−1.50	2.50	3.962E-12	0.00	3824	242	3957	160	4080	44	4080	44	1
M3	627	−1.50	3.00	4.405E-13	0.00	4810	117	4612	78	4716	58	4672	67	2
M3	650	−1.50	2.75	1.576E-12	0.00	4401	145	4276	71	4323	41	4306	52	2
M3	659	−1.50	2.75	1.330E-12	0.00	3825	245	4347	73	4384	45	4370	56	2
M3	675	−1.50	2.50	2.309E-12	0.00	3946	222	4235	78	4169	40	4191	53	2
M13	I2	−1.50	3.00	7.312E-13	0.03	4815	120	4821	73	4782	51	4798	60	2
M13	I18	−1.50	3.00	1.044E-12	0.03	4613	135	4634	78	4615	51	4623	62	2
M13	I23	−1.50	3.00	2.161E-12	0.03	4445	148	4547	71	4525	45	4534	55	2
M13	I24	−1.50	2.75	3.202E-12	0.03	4406	149	4382	76	4395	45	4390	57	2
M13	I48	−1.50	2.00	1.011E-11	0.03	<3500	—	3771	264	3940	44	3940	44	1
M13	II67	−1.50	2.00	9.800E-11	0.020	<3500	—	3786	242	3903	43	3903	43	1
M13	II76	−1.50	2.75	4.887E-12	0.03	4117	173	4179	91	4240	42	4221	57	2
M13	II90	−1.50	2.00	8.592E-12	0.03	3653	270	3800	198	3929	44	3929	44	1
M13	III18	−1.50	2.75	3.768E-12	0.03	4206	165	4292	68	4277	38	4282	49	2
M13	III56	−1.50	2.50	8.403E-12	0.03	4004	204	3909	287	4023	41	4023	41	1
M13	III63	−1.50	2.50	7.319E-12	0.03	4039	197	4033	76	4101	36	4079	49	2
M13	III73	−1.50	2.75	6.056E-12	0.03	3935	213	4142	89	4195	44	4177	59	2
M13	IV25	−1.50	3.50	9.431E-12	0.03	3856	173	<3500	—	3793	114	3793	114	1
M67	84	−0.08	2.50	2.337E-11	0.06	4805	130	4759	72	4740	53	4748	61	2
M67	94	−0.08	3.25	2.236E-12	0.06	6143	147	6154	106	6139	103	6146	116	3
M67	105	−0.08	2.00	3.534E-11	0.06	4620	146	4450	77	4453	48	4452	59	2
M67	108	−0.08	2.00	7.052E-11	0.06	4250	182	4192	77	4237	39	4222	52	2
M67	115	−0.08	3.25	2.674E-12	0.06	6070	140	5993	101	5993	96	6013	109	3
M67	117	−0.08	3.00	3.117E-12	0.06	5421	139	5262	83	5208	75	5275	92	3
M67	141	−0.08	2.50	2.586E-11	0.06	4832	127	4775	71	4740	53	4755	61	2
M67	151	−0.08	2.50	2.503E-11	0.06	4878	135	4815	71	4792	51	4802	59	2

Table 7. continued

GC	ID	[Fe/H]	log(g)	$F_{\rm Bol}$	$E(B-V)$	T_J	ΔT_J	T_H	ΔT_H	T_K	ΔT_K	$T_{\rm mean}$	$\Delta T_{\rm mean}$	n
M67	164	−0.08	2.50	2.474E-11	0.06	4716	149	4706	77	4693	55	4698	64	2
M67	170	−0.08	2.00	7.033E-11	0.06	4271	177	4249	72	4272	36	4264	48	2
M67	193	−0.08	2.75	4.670E-12	0.06	4997	133	4917	80	4918	61	4918	69	2
M67	223	−0.08	2.50	2.407E-11	0.06	4809	128	4748	73	4693	55	4717	63	2
M67	224	−0.08	2.75	2.031E-11	0.06	4689	153	4701	77	4704	56	4703	65	2
M67	231	−0.08	2.75	9.721E-12	0.06	5014	132	4841	72	4830	54	4869	75	3
M67	244	−0.08	2.75	1.752E-11	0.06	5149	140	5103	79	5045	62	5086	83	3
M67	I17	−0.08	3.00	4.120E-12	0.06	4899	144	4963	79	4909	61	4933	69	2
M67	I22	−0.08	3.00	2.411E-12	0.06	4996	145	5060	77	5059	64	5059	70	2
M67	III34	−0.08	2.75	1.223E-11	0.06	4577	148	4660	76	4683	54	4673	63	2
M67	IV20	−0.08	2.75	1.387E-11	0.06	4567	149	4619	73	4632	50	4627	59	2
M67	IV77	−0.08	3.00	2.551E-12	0.06	4967	144	4998	78	4999	62	4999	69	2
M67	IV81	−0.08	3.00	2.554E-12	0.06	5373	138	5385	89	5370	78	5376	96	3
M71	B	−0.94	1.50	3.762E-11	0.25	<3500	—	<3500	—	3589	72	3589	72	1
M71	A4	−0.94	1.75	1.589E-11	0.25	<3500	—	3780	73	3915	68	3915	68	1
M71	A6	−0.94	1.75	1.419E-11	0.25	3563	212	3778	72	3870	72	3870	72	1
M71	S	−0.94	2.00	6.328E-12	0.25	4010	213	4063	66	4139	36	4112	47	2
M71	A9	−0.94	2.00	6.700E-12	0.25	3577	228	3906	80	4008	58	4008	58	1
M71	N	−0.94	2.50	2.798E-12	0.25	4773	135	4787	72	4796	52	4792	60	2
M71	A7	−0.94	2.00	2.984E-12	0.25	4106	199	4360	71	4376	42	4370	53	2
M71	A5	−0.94	2.50	2.285E-12	0.25	4310	160	4494	74	4488	47	4490	57	2
M71	X	−0.94	3.00	1.004E-12	0.25	4997	145	5062	82	5120	61	5095	70	2
M71	A3	−0.94	3.00	9.522E-13	0.25	5057	140	5119	86	5109	62	5102	86	3
M71	C	−0.94	2.50	1.044E-12	0.25	4858	125	4821	72	4797	52	4807	60	2
M71	A2	−0.94	2.50	9.553E-13	0.25	4648	143	4651	75	4657	53	4655	62	2
M71	18	−0.94	2.50	1.079E-12	0.25	4687	144	4762	74	4805	53	4787	62	2
M71	19	−0.94	3.00	9.734E-13	0.25	5181	142	5220	89	5255	74	5226	94	3
M71	21	−0.94	2.00	5.144E-12	0.25	4269	166	4296	64	4320	39	4311	48	2
M71	29	−0.94	1.50	4.899E-11	0.25	3573	198	3504	50	3574	40	3574	40	1
M71	30	−0.94	1.75	1.939E-11	0.25	3805	264	3795	69	3897	56	3897	56	1
M71	45	−0.94	1.75	1.440E-11	0.25	3706	259	3770	76	3892	54	3892	54	1
M71	46	−0.94	1.75	1.589E-11	0.25	3588	226	3747	86	3874	54	3874	54	1
M71	75	−0.94	2.75	7.436E-13	0.25	4920	131	4740	77	4816	54	4785	63	2
M71	76	−0.94	2.50	1.565E-12	0.25	4567	136	4590	71	4589	48	4589	57	2
M71	77	−0.94	1.75	1.082E-11	0.25	3693	257	3788	71	3906	56	3906	56	1
M71	78	−0.94	2.00	6.334E-12	0.25	4289	161	4291	65	4300	38	4297	48	2
M71	79	−0.94	2.50	1.801E-12	0.25	4353	154	4475	76	4533	44	4512	56	2
M71	113	−0.94	1.75	1.476E-11	0.25	<3500	—	3632	109	3808	66	3808	66	1
M92	III13	−2.30	2.50	7.973E-12	0.02	3945	201	4033	200	4146	50	4123	80	2
M92	VII18	−2.30	2.50	6.982E-12	0.02	4199	162	4174	112	4222	50	4207	69	2
M92	X49	−2.30	2.50	6.478E-12	0.02	4306	140	4216	105	4279	41	4261	59	2
M92	III65	−2.30	2.75	5.074E-12	0.02	4420	142	4309	86	4366	49	4345	62	2
M92	XII8	−2.30	2.75	3.343E-12	0.02	4367	144	4397	92	4442	54	4425	68	2
M92	XI19	−2.30	2.75	3.062E-12	0.02	4460	140	4368	90	4433	54	4409	68	2
M92	II70	−2.30	2.75	2.511E-12	0.02	4569	122	4522	82	4537	48	4531	61	2
M92	III82	−2.30	3.00	1.866E-12	0.02	4647	131	4601	83	4575	51	4585	63	2
M92	IV10	−2.30	3.00	1.709E-12	0.02	4510	137	4532	81	4567	51	4553	63	2
M92	IV2	−2.30	3.00	1.536E-12	0.02	4639	133	4576	82	4619	54	4602	65	2
M92	IV114	−2.30	3.50	1.113E-12	0.02	4628	133	4613	91	4678	62	4652	74	2
M92	III4	−2.30	3.50	7.729E-13	0.02	5029	131	4963	98	4993	75	4992	96	3
M92	II12	−2.30	3.50	5.119E-13	0.02	4799	133	4924	99	4923	74	4923	85	2
47Tuc	1406	−0.90	2.75	1.907E-12	0.04	4364	152	4389	73	4399	44	4395	55	2
47Tuc	1407	−0.90	2.75	1.293E-12	0.04	4475	151	4546	66	4550	45	4548	54	2
47Tuc	1414	−0.90	3.00	7.420E-13	0.04	4879	131	4837	74	4844	56	4841	64	2
47Tuc	1421	−0.90	1.50	3.504E-11	0.04	<3500	—	<3500	—	3556	60	3556	60	1
47Tuc	1425	−0.90	2.75	9.307E-13	0.04	4584	134	4620	72	4615	49	4617	58	2
47Tuc	1505	−0.90	1.75	9.629E-12	0.04	3648	247	3835	71	3925	58	3925	58	1
47Tuc	1510	−0.90	2.00	8.385E-12	0.04	4000	210	3989	76	4052	49	4052	49	1
47Tuc	1513	−0.90	2.00	5.731E-12	0.04	4221	173	4163	77	4204	41	4190	54	2
47Tuc	1518	−0.90	2.75	2.598E-12	0.04	4385	157	4456	78	4490	46	4477	58	2
47Tuc	1602	−0.90	2.75	2.081E-12	0.04	4669	138	4610	72	4590	49	4598	58	2
47Tuc	1603	−0.90	1.50	1.506E-11	0.04	3734	261	3674	88	3799	42	3799	42	1
47Tuc	1604	−0.90	2.50	3.198E-12	0.04	4272	158	4216	77	4247	39	4237	52	2
47Tuc	2416	−0.90	2.00	4.959E-12	0.04	4039	204	4040	66	4104	53	4075	59	2
47Tuc	2426	−0.90	1.75	9.992E-12	0.04	3747	267	3855	73	3940	40	3940	40	1

Table 7. continued

GC	ID	[Fe/H]	log(g)	$F_{\rm Bol}$	$E(B-V)$	T_J	ΔT_J	T_H	ΔT_H	T_K	ΔT_K	$T_{\rm mean}$	$\Delta T_{\rm mean}$	n
47Tuc	2525	−0.90	2.00	5.568E-12	0.04	4215	174	4181	78	4217	41	4205	54	2
47Tuc	2603	−0.90	2.50	3.630E-12	0.04	4165	174	4170	77	4210	41	4196	54	2
47Tuc	2605	−0.90	2.00	5.275E-12	0.04	4304	149	4250	71	4204	41	4221	52	2
47Tuc	3407	−0.90	2.50	3.187E-12	0.04	4098	190	4225	77	4307	38	4280	51	2
47Tuc	3410	−0.90	2.50	2.492E-12	0.04	4374	152	4354	71	4368	42	4363	53	2
47Tuc	3501	−0.90	1.75	9.431E-12	0.04	3790	268	3892	77	3967	32	3967	42	1
47Tuc	3512	−0.90	1.50	2.207E-11	0.04	<3500	—	3504	42	3671	42	3671	42	1
47Tuc	4411	−0.90	2.75	9.268E-13	0.04	4570	137	4578	70	4624	51	4605	59	2
47Tuc	4415	−0.90	2.50	4.538E-12	0.04	4620	143	4692	79	4696	57	4694	66	2
47Tuc	4417	−0.90	3.00	7.780E-13	0.04	4914	142	4965	83	4983	66	4975	74	2
47Tuc	4418	−0.90	1.75	9.454E-12	0.04	3649	246	3835	71	3940	50	3940	50	1
47Tuc	4503	−0.90	2.00	5.361E-12	0.04	4255	170	4289	65	4314	39	4305	49	2
47Tuc	4603	−0.90	2.00	8.541E-12	0.04	3788	269	3986	76	4052	48	4052	48	1
47Tuc	5309	−0.90	1.75	8.685E-12	0.04	3621	241	3870	75	3983	52	3983	52	1
47Tuc	5312	−0.90	1.75	9.396E-12	0.04	3679	254	3821	69	3930	50	3930	50	1
47Tuc	5404	−0.90	2.50	3.186E-12	0.04	4480	151	4515	70	4533	44	4526	54	2
47Tuc	5406	−0.90	2.50	3.944E-12	0.04	4165	174	4130	74	4210	41	4181	53	2
47Tuc	5422	−0.90	2.00	6.072E-12	0.04	3915	228	4040	65	4076	31	4064	42	2
47Tuc	5427	−0.90	2.50	3.460E-12	0.04	4326	141	4207	78	4240	40	4229	53	2
47Tuc	5527	−0.90	2.75	1.573E-12	0.04	4406	157	4488	75	4498	46	4494	57	2
47Tuc	5529	−0.90	1.50	1.526E-11	0.04	<3500	—	3631	84	3792	42	3792	42	1
47Tuc	5627	−0.90	2.00	5.423E-12	0.04	4019	213	4122	72	4204	41	4174	52	2
47Tuc	5739	−0.90	2.00	6.586E-12	0.04	3903	232	3980	77	4062	48	4062	48	1
47Tuc	6407	−0.90	2.50	3.439E-12	0.04	4409	154	4352	71	4413	46	4389	56	2
47Tuc	6408	−0.90	2.50	3.844E-12	0.04	4120	181	4152	76	4247	39	4215	52	2
47Tuc	6502	−0.90	3.00	8.155E-13	0.04	5063	136	5159	88	5162	64	5140	87	3
47Tuc	6509	−0.90	2.75	1.531E-12	0.04	4367	157	4446	79	4527	44	4498	57	2
47Tuc	7320	−0.90	1.50	2.087E-11	0.04	<3500	—	<3500	—	3615	54	3615	54	1
47Tuc	7502	−0.90	2.75	1.120E-12	0.04	4530	142	4572	68	4542	45	4554	54	2
47Tuc	7507	−0.90	2.75	1.197E-12	0.04	4853	126	4702	78	4669	54	4683	64	2
47Tuc	8406	−0.90	2.00	7.046E-12	0.04	3856	246	3991	75	4027	48	4027	48	1
47Tuc	8416	−0.90	2.75	1.873E-12	0.04	4557	130	4470	76	4464	49	4466	60	2
47Tuc	8517	−0.90	2.00	4.559E-12	0.04	4069	205	4204	78	4252	47	4234	59	2
47Tuc	8518	−0.90	2.75	2.461E-12	0.02	4574	129	4549	66	4520	44	4532	53	2
ngc1261	3	−1.25	2.00	1.894E-12	0.01	3576	238	3780	179	3906	50	3906	50	1
ngc1261	9	−1.25	2.00	2.875E-12	0.01	4259	150	3940	84	3926	52	3926	52	1
ngc1261	10	−1.25	2.00	2.052E-12	0.01	3653	264	3812	75	3916	51	3916	51	1
ngc1261	11	−1.25	2.00	1.010E-12	0.01	4118	178	4078	68	4098	54	4089	60	2
ngc1261	52	−1.25	2.00	1.459E-12	0.01	4114	183	4113	73	4139	56	4128	63	2
ngc1261	81	−1.25	2.50	1.648E-12	0.01	4430	143	4213	79	4218	43	4216	56	2
ngc288	C19	−1.37	2.75	4.718E-13	0.02	4726	137	4736	78	4751	54	4745	64	2
ngc288	C20	−1.37	2.00	3.453E-12	0.02	4086	185	4010	75	4073	52	4047	61	2
ngc288	C23	−1.37	2.75	3.931E-13	0.02	4874	125	4776	74	4767	53	4771	62	2
ngc288	C32	−1.37	2.75	2.438E-13	0.02	4912	130	4827	75	4829	55	4828	63	2
ngc288	C33	−1.37	2.50	1.030E-12	0.02	4303	156	4410	77	4445	49	4431	60	2
ngc288	C36	−1.37	2.50	1.221E-12	0.02	4394	153	4383	75	4420	48	4406	59	2
ngc288	A77	−1.37	2.00	2.934E-12	0.02	4353	139	4180	80	4208	43	4198	56	2
ngc288	A78	−1.37	2.00	3.858E-12	0.02	4250	156	4080	69	4101	44	4093	54	2
ngc288	A80	−1.37	2.50	1.169E-12	0.02	4582	127	4486	77	4518	45	4506	57	2
ngc288	A96	−1.37	2.00	4.967E-12	0.02	4112	175	3955	88	4028	40	4028	40	1
ngc288	A194	−1.37	2.00	2.885E-12	0.02	4393	146	4247	75	4257	37	4254	50	2
ngc288	A231	−1.37	2.50	1.640E-12	0.02	4638	137	4444	80	4454	50	4450	62	2
ngc288	A245	−1.37	2.50	2.027E-12	0.02	4398	149	4331	70	4359	42	4349	53	2
ngc288	A260	−1.37	1.50	8.875E-12	0.02	3500	150	3589	116	3749	54	3749	54	1
ngc362	I2	−0.98	2.75	8.471E-13	0.04	4573	131	4562	68	4549	45	4554	54	2
ngc362	I23	−0.98	2.50	2.108E-12	0.04	4363	144	4263	70	4294	37	4283	48	2
ngc362	I44	−0.98	2.50	2.870E-12	0.04	4384	148	4291	65	4288	37	4289	47	2
ngc362	I52	−0.98	2.75	4.060E-13	0.04	4478	151	4515	71	4581	48	4554	57	2
ngc362	II20	−0.98	2.00	4.803E-12	0.04	3644	255	3881	77	3976	53	3976	53	1
ngc362	II40	−0.98	2.75	4.568E-13	0.04	4774	128	4702	79	4706	57	4704	66	2
ngc362	II43	−0.98	2.75	1.310E-12	0.04	4687	137	4602	71	4615	50	4610	59	2
ngc362	II47	−0.98	2.75	8.099E-13	0.04	4603	139	4740	75	4725	56	4731	64	2
ngc362	II49	−0.98	2.50	1.188E-12	0.04	4275	165	4393	74	4422	47	4411	57	2
ngc362	III4	−0.98	2.50	1.690E-12	0.04	4288	158	4331	67	4294	37	4307	48	2
ngc362	III11	−0.98	2.00	7.639E-12	0.04	<3500	—	3774	76	3852	50	3852	50	1
ngc362	III25	−0.98	2.50	1.858E-12	0.04	4370	150	4334	69	4369	42	4356	52	2
ngc362	III37	−0.98	2.50	2.867E-12	0.04	4380	149	4304	65	4314	39	4310	49	2
ngc362	III39	−0.98	2.00	6.107E-12	0.04	3552	215	3927	82	3993	51	3993	51	1
ngc362	III44	−0.98	2.00	4.783E-12	0.04	3997	211	3940	81	4012	49	4012	49	1
ngc362	III63	−0.98	2.00	6.000E-12	0.04	3661	253	3806	68	3905	48	3905	48	1

Table 7. continued

GC	ID	[Fe/H]	log(g)	$F_{\rm Bol}$	$E(B-V)$	T_J	ΔT_J	T_H	ΔT_H	T_K	ΔT_K	$T_{\rm mean}$	$\Delta T_{\rm mean}$	n
ngc362	III70	−0.98	2.00	4.3632E-12	0.04	3902	242	4108	71	4132	45	4123	55	2
ngc362	IV84	−0.98	2.00	3.896E-12	0.04	<3500	—	3950	81	4021	49	4021	49	1
ngc362	IV91	−0.98	2.50	1.981E-12	0.04	4210	175	4366	72	4382	44	4376	55	2
ngc362	IV100	−0.98	2.00	5.923E-12	0.04	<3500	—	3702	156	3856	55	3856	55	1
ngc362	V2	−0.98	1.50	7.716E-12	0.04	<3500	—	3777	69	3779	50	3779	50	1

In order to estimate the error of the mean temperature, a linear transmission of the errors was considered, given that the errors in each band are not totally independent:

$$\Delta T_{\rm IRFM} = \frac{N}{\sum\limits_{i=J,H,K,L} \frac{1}{\Delta T_i}}, \quad (7)$$

where N is the number of bands considered and the error in the temperature of each band is defined by

$$(\Delta T_i)^2 = \left[\frac{\partial T_i}{\partial[q(\lambda_i)R(\lambda_i)]}\right]^2 (\Delta[q(\lambda_i)R(\lambda_i)])^2 + \left[\frac{\partial T_i}{\partial[{\rm Fe/H}]}\right]^2 (\Delta[{\rm Fe/H}])^2 + \left[\frac{\partial T_i}{\partial \log(g)}\right]^2 (\Delta \log(g))^2. \quad (8)$$

The quantities in square brackets have been estimated by considering finite-difference interpolation with the help of grids of values similar to those displayed in Tables 1–4 with a finer spacing. Over 5000 K, the temperatures in the three (four) bands enter the average with similar weight. In that range, the assignment of weights automatically takes into account the uneven sensitivity of the IRFM in the different bands and the individual quality of IR photometry. However, below 5000 K only T_H, T_K and $T_{L'}$ have been considered in the average, since R_J is a very insensitive indicator of temperature for the cooler stars. Under 4000 K, only T_K and $T_{L'}$ have been considered. This is due to the fact that the coolest models show in the H band a local maximun of flux which is not observed in IR spectra (Lançon & Rocca-Volmerange 1992).

The mean error in the final temperatures is around $1-2\%$. Note however, that the uncertainties in the temperatures derived under 4000 K are greater than the errors determined from Eq. (8) due to the model imperfections in this range caused by the absence of important sources of opacity associated with certain molecules. Likewise, the IRFM is difficult to apply at temperatures above 8000 K because, as these stars emit a substantial proportion of energy at short wavelengths, the correction for insterstellar extinction and the determination of the bolometric flux are rather uncertain. For these reasons, the temperatures outside the range 4000 K $< T_{\rm eff} <$ 8000 K have a lower level of accuracy, and the error-bars quoted in Tables 6 and 7 have to be considered, in some cases, as lower estimates.

We show in Figs. 5 and 6 the difference between T_J, T_H, T_K and $T_{L'}$, and the average temperature adopted.

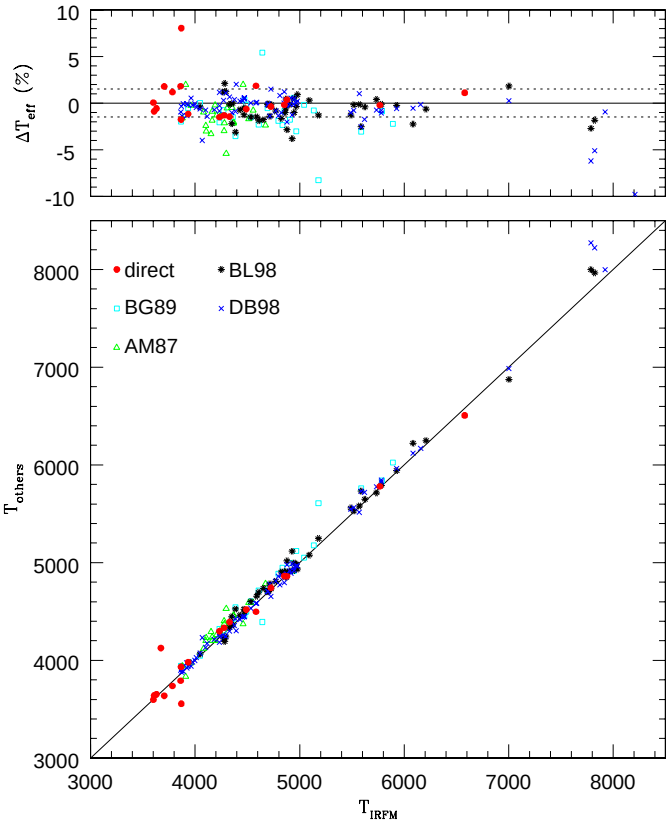

Fig. 7. Differences between the temperatures derived in this work ($T_{\rm IRFM}$) and those derived by other authors. circles: Direct measurements: C76, R80, BR87, H89, M91, and WF87; squares: Bell & Gustafsson (1989), triangles: Arribas & Martínez-Roger (1987). stars: Blackwell & Lynas-Gray (1998). In the upper figure the lines corresponding to the mean internal error of the work (± 1.5%) are shown

The individual residuals reveal that the dispersion is compatible with the estimated errors derived from the uncertainties in the input parameters of the IRFM. They follow approximately a normal distribution both with temperature and metallicity. As expected, the uncertainties are greater for temperatures obtained from R_J factors, due to the lower sensitivity of the IRFM in this band and the greater photometric error in the measurement of magnitude J. The consistency of T_J and T_H is good over 4500 K; however, under this temperature noteworthy discrepancies appear to be due to the fact that R_J- and R_H-factors lose their sensitivity to temperature in this range.

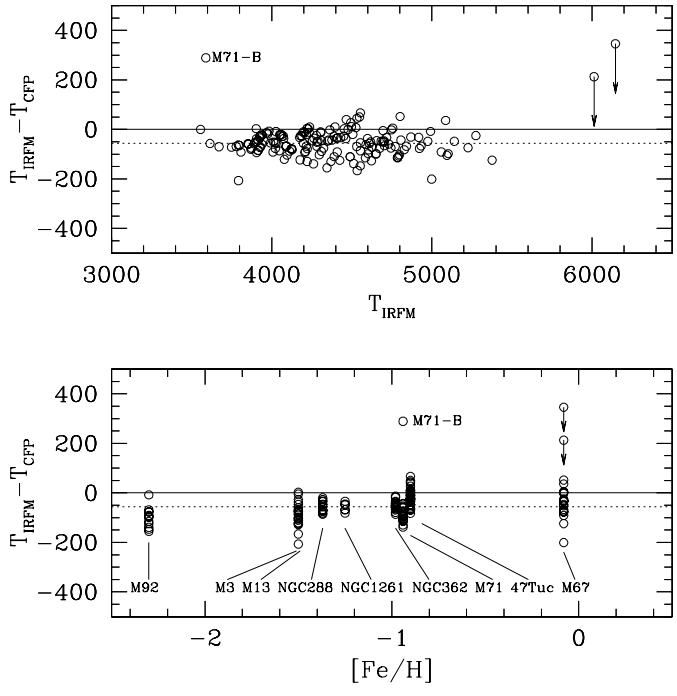

Fig. 8. Differences between the temperatures derived in this work ($T_{\rm IRFM}$) and those derived by Frogel et al. (1979, 1981, 1983) and Cohen et al. (1978) ($T_{\rm CFP}$). Top: Differences against $T_{\rm IRFM}$. Bottom: Differences against metallicity. The differences are consistent with a zero-point offset amounting to 56 K (dotted line)

Table 8. Comparison between the temperatures derived in the present work (Col. 3) and those derived by *direct* methods (Col. 2). When several direct measurements were available we have considered the average value. The temperatures of the Sun and Procyon, measured in Paper I, are also listed. The mean difference $T_{\rm direct} - T_{\rm IRFM}$ is 3 ± 51 K

Star	$T_{\rm direct}$ (K)	$T_{\rm IRFM}$ (K)	ΔT (K) (%)
HR 7635	3556	3867	–8.7
HR 8775	3598	3600	–0.1
HR 911	3638	3704	–1.8
HR 4902	3639	3607	+0.9
HR 2286	3652	3631	+0.6
HR 337	3738	3783	–1.2
HR 3705	3791	3861	–1.8
HR 1457	3934	3866	+1.7
HR 6705	3980	3934	+1.2
HR 5301	4125	3672	+10.1
HR 5340	4297	4233	+1.5
HR 603	4333	4277	+1.3
HR 165	4392	4329	+1.4
HR 168	4497	4582	–1.9
HR 617	4519	4490	+0.6
HR 7949	4743	4725	+0.4
HR 2990	4863	4854	+0.2
HR 7776	4860	4878	–0.4
Sun	5780	5767	+0.2
HR 2943	6506	6579	–1.1

Table 9. Comparison between the temperatures derived in the present work (Col. 2) and those derived by Arribas & Martínez-Roger (1987) (Col. 3). The mean difference $T_{\rm IRFM} - T_{\rm AM89}$ is −1.3 ± 1.4% (without M3-53)

Star	$T_{\rm IRFM}$ (K)	$T_{\rm AM87}$ (K)	ΔT (K)	ΔT (K) (%)
M3-26	3877	3940	–63	–1.6
M3-33	4101	4200	–99	–2.4
M3-46	4459	4370	+89	+2.0
M3-53	4297	4530	–233	–5.4
M3-68	4354	4375	–21	–0.5
M3-72	4276	4404	–128	–3.0
M3-155	4555	4590	–35	–0.7
M3-311	4206	4260	–54	–1.3
M3-313	4514	4590	–76	–1.7
M3-428	4239	4300	–61	–1.4
M3-444	4163	4200	–37	–0.9
M3-464	4106	4230	–124	–3.0
M3-496	4153	4290	–137	–3.3
M3-525	3959	3970	–11	–0.3
M3-557	4162	4240	–78	–1.9
M3-567	4279	4370	–91	–2.1
M3-586	3911	3834	+77	+2.0
M3-605	4365	4460	–95	–2.2
M3-617	4080	4120	–40	–1.0
M3-627	4672	4784	–112	–2.4
M3-650	4306	4330	–24	–0.6
M3-659	4370	4460	–90	–2.1
M3-675	4191	4200	–9	–0.2

6. Comparison with other determinations

In this section, we provide the comparison of our temperatures with those derived by other authors for common stars in the sample. We show differences found in Figs. 7 and 8. Furthermore, a detailed analysis of the scale of temperatures derived from the present work will be given in a subsequent paper by considering the mean relations $T_{\rm eff}$: [Fe/H] and the $UBVRIJHK$ and *uvby* photometric colours.

Direct methods

There is a group of 18 giant stars in the sample whose diameters have been measured by optical methods (Code et al. (1976; C76), Ridgway et al. (1980; R80), Di Benedetto & Rabbia (1987; BR87), Hutter et al. (1989; H89), Mozurkewich et al. (1991; M 91), and White & Feiermann (1987; WF87)). In Table 8, we provide the comparison between IRFM temperatures and those obtained considering their measured angular diameters and bolometric fluxes. If we consider the typical errors of both the direct method and the IRFM the differences observed are within the error-bars. Excluding HR 7635 and HR 5301, the average difference $T_{\rm direct} - T_{\rm IRFM}$

amounts to $0.06 \pm 1.25\%$. Moreover, no apparent trend of the differences with temperature is observed.

Arribas & Martínez-Roger (1987, AM87)

There are 23 stars of M 3 from the article of Arribas & Martínez-Roger (1987, AM87), based on the application of the IRFM and using the empirical absolute flux calibration of the IR flux of Vega derived by Mountain et al. (1985), and the models of Kurucz (1979) and Gustaffson et al. (1975), which are common with our work (Table 9). Temperatures derived by AM87 are, on average, 55 K hotter, with a standard deviation amounting to 59 K. No obvious trend with temperature can be seen in the differences (Fig. 7). The shift in temperatures, amounting to 1.3%, might be explained by taking into account the different absolute flux calibration, and the improvement of Kurucz's models.

Bell & Gustafsson (1989, BG89)

This work contains 25 stars in common with the present sample. BG89 temperatures are based on the IRFM corrected with IR synthetic colours. The differences listed in Table 10 are compatible with a zero-point shift of 65 K (T_{BG89} are hotter) or $1.3 \pm 1.1\%$. These differences are probably connected with the differences in the bolometric fluxes adopted in both works (Sect. 4.2).

Blackwell & Lynas-Gray (1998; BL98)

This extensive study provides temperatures for 420 stars (A0–K3) with luminosity classes between II and V, incorporating previous results of similar accuracy (Blackwell et al. 1990 and Blackwell & Lynas-Gray 1994). It is a good source for comparison, given that it is based on the IRFM with the same models adopted in the present work, the basic differences being the calibration of the IR flux of Vega, and the scale of bolometric fluxes. In Fig. 7, we show the differences in temperature for the 50 Population I giants common to the present sample. On average, $T_{\rm BL98}$ are 36 ± 67 K hotter than ours; no apparent trend of the differences versus $T_{\rm eff}$ is seen. This shift in temperature ($0.70\% \pm 1.25\%$) is compatible with the difference in the bolometric fluxes (around 1.5%) found in Sect. 4.2.

Di Benedetto (1998; DB98)

This work reports on the implementation of the empirical surface brightness technique using Jonhson $(V-K)$ colours for 537 dwarf and giant stars A-K. There are 70 giant and subgiant stars of DB98 common both to Paper I and the present work. Below 7000 K, the agreement is fairly good. The DB98 temperatures are 12 K hotter with a dispersion of 42 K ($0.23 \pm 0.93\%$). However, for the four stars with $T_{\rm IRFM} > 7000$ K a difference of 400 $\pm$ 300 K is observed (the DB98 temperatures are hotter). This fact is probably related to the difficulty in estimating bolometric fluxes for early-type stars.

Table 10. Comparison between the temperatures derived in the present work (Col. 2) and those derived by Bell & Gustafsson (1989) (Col. 3). The mean difference $T_{\rm IRFM} - T_{\rm BG89}$ is -65 ± 56 K discarding HR 4247 and HR 5889

Star	$T_{\rm IRFM}$ (K)	$T_{\rm BG89}$ (K)	ΔT (K)	ΔT (K) (%)
HR 0617	4490	4499	–9	–0.2
HR 1457	3866	3943	–77	–2.0
HR 2990	4854	4896	–42	–0.9
HR 5340	4233	4321	–88	–2.1
HR 6705	3934	3955	–21	–0.5
HR 0219	5789	5839	–49	–0.8
HR 0434	4042	4046	+0	+0.0
HR 0464	4359	4425	–66	–1.5
HR 1907	4693	4719	–26	–0.6
HR 3323	5136	5176	–40	–0.8
HR 3403	4387	4542	–155	–3.5
HR 4247	4643	4392	+251	+5.4
HR 4932	5043	5052	-9	-0.2
HR 4983	5892	6024	–132	–2.2
HR 5429	4271	4303	–32	–0.7
HR 5889	5180	5608	–428	–8.2
HR 6220	4942	4913	+29	+0.6
HR 6603	4533	4603	–70	–1.5
HR 6770	4969	5120	–151	–3.0
HR 6869	4835	4949	–114	–2.3
HR 7429	4473	4456	+17	+0.4
HR 7615	4796	4887	–91	–1.9
HR 7957	4908	4996	–88	–1.8
HR 8255	4609	4715	–106	–2.2
HR 4883	5589	5841	–172	–3.1

Cohen et al. (1978), Frogel et al. (1979, 1981, 1983); CFP

The scale of temperatures defined by CFP has been adopted as standard in many studies devoted to the analysis of chemical abundances of giant stars and the calibration of stellar evolution models of the RGB. In the series of papers above mentioned, the authors provide effective temperatures for an extended sample of Red Giant Branch stars of globular clusters. The effective temperatures derived by CFP are based on atmosphere models and multicolour photometry (a brief description of the method used to derive temperatures is detailed in Frogel et al. 1981). In Fig. 8, we show the differences observed between $T_{\rm IRFM}$ and $T_{\rm CFP}$. In average, $T_{\rm CFP}$ are 56 K hotter than $T_{\rm IRFM}$

with a dispersion of 46 K. No apparent trend of the differences with $T_{\rm eff}$ or [Fe/H] is appreciated.

In summary, temperatures derived here are comparable with those derived by other authors. On the one hand, the differences and the dispersion of the differences found with other works based on the IRFM are within the errorbars of both accidental errors (i.e. uncertainty on the bolometric and monochromatic fluxes and other input parameters of the IRFM) and systematic errors (i.e. uncertainty in the absolute flux calibration as commented in Sect. 4.1 and different grids of model fluxes). On the other hand, the differences and the dispersion of the differences found with direct methods and surface brightness method are consistent with the combination of our internal error estimates and theirs.

7. Summary

The IRFM has been applied to a sample of approximately 500 giant stars later than F0, which cover the metallicity range (0.5, −3.5). Near-IR monochromatic fluxes have been used in order to derive T_J, T_H, T_K and $T_{L'}$ for each star. The uncertainties in the input parameters needed to apply the IRFM and the induced errors on the three/four temperatures derived have been computed. The consistency of the temperatures derived in the three different bands is fairly good above 4000 K. The final temperature for each star in the sample has been derived considering the mean of T_J, T_H, T_K and $T_{L'}$ weighted with the inverse of their errors. From the analysis of the systematic errors associated with the uncertainty in the absolute flux calibration in the near-IR, the expected indeterminacy of the zero point of the temperature scale should be around 1%. However, the good agreement between the IRFM and direct temperatures of a sample of 18 giant stars suggests a lower uncertainty. The internal estimated precision for the final temperatures, considering the effect of accidental errors, is around 1.5%. The comparison with other works also based on semi-empirical and empirical methods shows slight discrepancies which may be explained by considering the internal errors affecting the determination of temperatures.

Acknowledgements. We are grateful to the referee, Dr. Lynas-Gray, for his careful assessment of the paper and for many comments and suggestions which have certainly improved the final version. We are also grateful to Terry Mahoney for correcting this paper for English and style. We have made use for this research of the SIMBAD database, operated at CDS, Strasbourg, France.

References

Alonso A., Arribas S., Martínez-Roger C., 1994a, A&A 282, 684 (Paper II)
Alonso A., Arribas S., Martínez-Roger C., 1994b, A&AS 107, 365
Alonso A., Arribas S., Martínez-Roger C., 1995, A&A 297, 197 (Paper III)
Alonso A., Arribas S., Martínez-Roger C., 1996a, A&AS 117, 227 (Paper I)
Alonso A., Arribas S., Martínez-Roger C., 1996b, A&A 313, 873
Alonso A., Arribas S., Martínez-Roger C., 1998, A&AS 131, 209 (Paper IV)
Anthony-Twarog B.J., Twarog B.A., 1994, AJ 107, 1577
Arribas S., Caputo F., Martínez-Roger C., 1991, A&AS 88, 19 (AM87)
Arribas S., Martínez-Roger C., 1987, A&A 178, 107
Bell R.A., Gustafsson B., 1989, MNRAS 236, 653 (BG89)
Bell R.A., 1992, MNRAS 257, 423
Bessell M.S., Castelli F., Plez B., 1998, A&A 333, 231 (BCP98)
Blackwell D.E., Petford A.D., Arribas S., Haddock D.J., Selby M.J., 1990, A&A 232, 396
Blackwell D.E., Petford A.D., 1991, A&A 250, 459
Blackwell D.E., Lynas-Gray A.E., 1994, A&A 282, 899
Blackwell D.E., Lynas-Gray A.E., 1998, A&AS 129, 505 (BL98)
Böhm-Vitense E., 1981, ARA&A 19, 295
Burstein D., Heiles C., 1982, AJ 87, 1165
Carney B.W., 1979, ApJ 233, 211
Cayrel de Strobel G., Soubiran C., Friel E.D., et al., 1997, A&AS 124, 299
Clark F.O., 1996, PLEXUS Version 2.1a, CD-ROM. Hanscom AFB, MA: Phillips Lab., Dir. Geophys., Air Force Mater. Command
Code A.D., Davis J., Bless R.C., Hanbury-Brown R., 1976, ApJ 203, 417 (C76)
Cohen J.G., Frogel J.A., Persson S.E., 1978, ApJ 222, 165
Crawford D.L., 1975, AJ 80, 955
Di Benedetto G.P., 1993, A&A 270, 315
Di Benedetto G.P., 1998, A&A 339, 858 (DB98)
Di Benedetto G.P., Rabbia Y., 1987, A&A 188, 114 (BR87)
Dyck H.M, van Belle G.T., Thompson R.R., 1998, AJ 116, 981
Dreiling L.A., Bell R.A., 1980, ApJ 241, 736
Flower P.J., 1996, ApJ 469, 365 (F96)
Frogel J.A., Persson S.E., Cohen J.G., 1979, ApJ 227, 499
Frogel J.A., Persson S.E., Cohen J.G., 1981, ApJ 246, 842
Frogel J.A., Persson S.E., Cohen J.G., 1983, ApJS 53, 713
Gustafsson B., Bell R.A., Eriksson K., Nordlund A., 1975, A&A 42, 407
Hakkila J., Myers J.M., Stidham B.J., Hartmann D.H., 1997, AJ 114, 2043
Hayes D.S., Latham D.W., 1975, ApJ 197, 593
Hutter D.J., Johnston K.J., Mozurkewich D., et al., 1989, ApJ 340, 1103 (H89)
Lançon A., Rocca-Volmerange B., 1992, A&AS 96, 593
Landolt-Börnstein, 1982, New Series, Gp VI, Vol. 2, Astronomy and Astrophysics, Subvolume C. Springer, Berlin-Heidelberg-New York
Kurucz R.L., 1993, CD-ROM # 13
Kurucz R.L., 1995, CD-ROM # 23
Malagnini M.L., Morossi C., Buser R., Parthasarathy M., 1992, A&A 267, 558

Morossi C., Franchini M., Malagnini M.L., et al., 1993, A&A 277, 173
Mozurkewich D., Johnston K.J., Simon R.S., et al., 1991, AJ 101, 2207 (M91)
Peterson C.J., 1986, PASP 98, 192
Petford A.D., Blackwell D.E. Booth A.J., et al., 1988, A&A 203, 341
Plez, B., Brett J.M., Nordlund Å., 1992, A&A 256, 551
Richichi A., Di Giacomo A., Lisi F., Calamai G., 1992, A&A 265, 535
Ridgway S.T., Joyce R.R., White N.M., Wing R.F., 1980, ApJ 235, 126 (R80)
Selby M.J., Hepburn I., Blackwell D.E., et al., 1988, A&AS 74, 127
Tüg H., White N.M., Lockwood G.W., 1977, A&A 61, 67
Walker R.G., Cohen M., 1992, An atlas of selected calibrated stellar spectra. NASA Contractor Report 177604, NASA Ames Research Center, Moffett Field. California 94035-1000
White N.M., Feierman B.H., 1987, AJ 94, 751 (WF87)